

(19)



Europäisches Patentamt  
European Patent Office  
Office européen des brevets



(11)

**EP 1 043 065 B1**

(12)

**EUROPEAN PATENT SPECIFICATION**

(45) Date of publication and mention  
of the grant of the patent:  
**01.09.2004 Bulletin 2004/36**

(51) Int Cl.7: **B01J 23/38, B01J 37/02,  
B01D 53/94, B01J 35/00  
// F01N3:20**

(21) Application number: **98957210.2**

(86) International application number:  
**PCT/JP1998/005526**

(22) Date of filing: **04.12.1998**

(87) International publication number:  
**WO 1999/032223 (01.07.1999 Gazette 1999/26)**

(54) **EXHAUST GAS CLEANING CATALYST, PROCESS FOR PRODUCING THE SAME, AND EXHAUST  
GAS CLEANING METHOD**

KATALYSATOR ZUM REINIGEN VON ABGAS, VERFAHREN ZU SEINER HERSTELLUNG UND  
VERFAHREN ZUM REINIGEN VON ABGAS

CATALYSEUR D'EPURATION DES GAZ D'ECHAPPEMENT, PROCEDE DE FABRICATION  
CORRESPONDANT ET PROCEDE D'EPURATION DES GAZ D'ECHAPPEMENT

(84) Designated Contracting States:  
**DE FR GB**

• **TSUJI, Shinji, Toyota Jidosha Kabushiki Kaisha  
Toyota-shi, Aichi-ken 471-8571 (JP)**

(30) Priority: **22.12.1997 JP 35389097  
20.05.1998 JP 13862098  
01.09.1998 JP 24748298**

(74) Representative:  
**Winter, Brandl, Fűrnliss, Hübner, Röss, Kaiser,  
Polte Partnerschaft  
Patent- und Rechtsanwaltskanzlei  
Alois-Steinecker-Strasse 22  
85354 Freising (DE)**

(43) Date of publication of application:  
**11.10.2000 Bulletin 2000/41**

(73) Proprietor: **TOYOTA JIDOSHA KABUSHIKI  
KAISHA  
Aichi-ken 471-8571 (JP)**

(56) References cited:  

|                         |                         |
|-------------------------|-------------------------|
| <b>EP-A- 0 666 103</b>  | <b>EP-A- 0 669 157</b>  |
| <b>WO-A-95/32790</b>    | <b>JP-A- 3 086 240</b>  |
| <b>JP-A- 5 293 383</b>  | <b>JP-A- 6 269 684</b>  |
| <b>JP-A- 7 068 174</b>  | <b>JP-A- 7 100 380</b>  |
| <b>JP-A- 9 103 651</b>  | <b>JP-A- 10 216 518</b> |
| <b>JP-A- 10 216 519</b> | <b>JP-A- 59 160 536</b> |
| <b>JP-A- 63 097 232</b> |                         |

(72) Inventors:  
• **HIRATA, Hirohito,  
Toyota Jidosha Kabushiki Kaisha  
Toyota-shi, Aichi-ken 471-8571 (JP)**

**EP 1 043 065 B1**

Note: Within nine months from the publication of the mention of the grant of the European patent, any person may give notice to the European Patent Office of opposition to the European patent granted. Notice of opposition shall be filed in a written reasoned statement. It shall not be deemed to have been filed until the opposition fee has been paid. (Art. 99(1) European Patent Convention).

## Description

## TECHNICAL FIELD

5 [0001] This invention relates to an exhaust-gases-purifying catalyst for purifying such toxic substances as hydrocarbons (HC), carbon monoxide (CO), and nitrogen oxides (NO<sub>x</sub>) contained in exhaust gases from an automotive engine or other internal combustion engines or boilers, a method of producing this catalyst and a method of purifying exhaust gases by using this catalyst.

## 10 TECHNICAL BACKGROUND

[0002] As catalysts for purifying exhaust gases from automotive engines, catalysts have been widely used in which such a noble metal as platinum (Pt), rhodium (Rh) and palladium (Pd) is loaded on a support formed of such a porous oxide as alumina (Al<sub>2</sub>O<sub>3</sub>). For example, a 3-way catalyst is formed by loading Pt and/or Rh on such a porous oxide as γ-Al<sub>2</sub>O<sub>3</sub>, and oxidizes HC and CO in the exhaust gases into innocuous entities and at the same time reduces NO<sub>x</sub> in the exhaust gases into innocuous entities. Pt, which is especially active, is mainly used as a noble metal.

15 [0003] Regarding the production of an exhaust-gases-purifying catalyst like this three-way catalyst, a porous oxide support powder or a porous oxide support coated on a honeycomb-shaped supporting base material is brought in contact with an aqueous solution of a noble metal chloride, a noble metal nitro complex, or a noble metal ammonium complex, and then dried and calcined. Thus, a noble metal is loaded. The noble metal loaded by this method is highly dispersed on an atomic level, and the resulting catalyst attains an extremely high catalytic activity.

20 [0004] On the other hand, carbon dioxide (CO<sub>2</sub>) in the exhaust gases from the internal combustion engines of automobiles, etc. has recently become a problem in view of global environmental conservation. What we call "lean burn", i.e., burning lean fuel in oxygen-excessive atmospheres is desired as a solution to this problem. The lean burn improves fuel consumption, and as a result the amount of fuel consumed is decreased and CO<sub>2</sub>, which is a combustion exhaust gas, can be suppressed from generating.

25 [0005] In this respect, the conventional 3-way catalysts aim to oxidize CO and HC and reduce NO<sub>x</sub> simultaneously into innocuous entities when the air-fuel ratio is at the ideal air-fuel ratio, i.e., at the stoichiometric point, and cannot exhibit sufficient reduction and removal of NO<sub>x</sub> in the exhaust gases in oxygen-excessive atmospheres at the time of lean burn. Hence, it has been desired to develop catalysts which are capable of purifying NO<sub>x</sub> adequately even in oxygen-excessive atmospheres.

30 [0006] Under these circumstances, the applicants et al of the present invention have proposed an exhaust-gases-purifying catalyst in which Pt and an NO<sub>x</sub> storage component such as Ba are loaded on a porous support formed of alumina, etc., for example, in Japanese Unexamined Patent Publication (KOKAI) No. 5-317,625. By using this catalyst for purifying exhaust gases and controlling the air-fuel ratio to change pulsatorily from the fuel-lean side to the stoichiometric point or the fuel-rich side, namely, to perform "fuel-rich spikes", NO<sub>x</sub> are adsorbed and stored by the NO<sub>x</sub> storage component on the fuel-lean side and the adsorbed NO<sub>x</sub> are released and react with reducing components such as HC and CO into innocuous entities at the stoichiometric point or on the fuel-rich side. Thus, NO<sub>x</sub> can be purified efficiently even in the case of lean burn.

35 [0007] In a method of producing an NO<sub>x</sub> storage and reduction type catalyst like this, a slurry including such a porous oxide as alumina and a binder is prepared and this slurry is coated on a honeycomb-shaped supporting base material formed of cordierite or a metal and calcined, thereby forming a coating layer. Next, the supporting base material having the coating layer thereon is immersed in a solution of a noble metal compound, thereby loading a noble metal, and then immersed in a solution of an NO<sub>x</sub> storage component, thereby loading the NO<sub>x</sub> storage component. Also known is another production method comprising preparing a slurry from a support powder in which an NO<sub>x</sub> storage component and a noble metal are loaded on alumina, etc., coating this slurry on a honeycomb supporting base material and calcining the material.

40 [0008] However, although the conventional 3-way catalysts and the NO<sub>x</sub> storage and reduction type catalysts exhibit superb catalytic activity in the initial stage of its use, they suffer from a drawback in that the catalytic activity gradually deteriorates as time passes. This degradation is particularly remarkable with the NO<sub>x</sub> storage and reduction type catalysts for purifying the exhaust gases from lean-burn engines. Our studies so far have clarified that the catalytic activity degradation with the passage of time is caused by the fact that since grains of noble metals, particularly Pt grow in fuel-lean oxygen-excessive atmospheres at high temperatures, the surface area of the noble metals decreases and consequently catalytic-activity sites decrease.

45 [0009] On the other hand, exhaust gases contain SO<sub>2</sub>, which is produced from a sulfur component of a fuel, and the SO<sub>2</sub> is oxidized and react with an NO<sub>x</sub> storage component on a catalyst, thereby producing sulfates. The sulfates do not decompose and are stable around exhaust gas temperatures. Accordingly, there arises a problem that the NO<sub>x</sub> storage ability of the NO<sub>x</sub> storage component gradually disappears and the NO<sub>x</sub> purifying ability gradually deteriorates.

This phenomenon is called sulfur poisoning of the NO<sub>x</sub> storage component.

[0010] DE-A-44 10 353 discloses the production of mixed noble metal catalysts by loading a colloid on an porous oxide support; a polymer protection agent is used in the production process.

5 [0011] WO 95/32790 describes loading of a colloidal suspension of a platinum alloy with at least one metal. Alloying is accomplished by thermal treatment or by colloidal methods.

[0012] The present invention has been developed in view of the aforementioned circumstances. It is a primary object of the present invention to suppress a decrease in catalytic activity by suppressing grain growth of a noble metal so as to improve the durability of 3-way catalytic activity and NO<sub>x</sub> conversion activity and provide an exhaust-gases-purifying catalyst with improved durability.

10 [0013] It is another object of the present invention to suppress sulfur poisoning of an NO<sub>x</sub> storage component in NO<sub>x</sub> storage and reduction type catalysts.

#### DISCLOSURE OF THE INVENTION

15 [0014] A catalyst for purifying exhaust gases recited in claim 1, which dissolves the above problem, is obtainable by loading on a porous oxide support a noble metal composite colloid composed of a plurality of noble metals and having a particle size of from 1 to 5 nm.

[0015] An embodiment of the catalyst for purifying exhaust gases is obtainable by loading the noble metal composite colloid on the surface of said porous oxide support and further loading an atomic-state noble metal in micro pores of said porous oxide support.

[0016] A further embodiment of the catalyst for purifying exhaust gases is obtainable by further loading on said porous oxide support an NO<sub>x</sub> storage component selected from the group consisting of alkali metals, alkaline-earth metals and rare-earth elements.

25 [0017] An exhaust-gases-purifying catalyst production method recited in claim 5, which is suitable to produce the embodiments of the exhaust-gases-purifying catalysts mentioned above, is characterized in comprising:

a separation step of taking a noble metal composite colloid composed of a plurality of noble metals and having a particle size of from 1 to 5 nm out of a polymer-protected noble metal composite colloid which is composed of a plurality of noble metals and protected by a polymeric material;

30 a solution preparation step of dispersing said noble metal composite colloid in water by using a surfactant so as to prepare a surfactant-protected noble metal composite colloidal solution; and

a noble-metal-colloid-loading step of bringing a porous oxide support in contact with said surfactant-to load a surfactant-protected noble metal composite colloid on said porous oxide support.

35 [0018] A preferred embodiment of the method of producing the catalyst comprises further an atomic-state-noble-metal-loading step of bringing the porous oxide support in contact with an aqueous solution of pyromellitic acid and a noble metal compound so as to load an atomic-state noble metal on the porous oxide support.

[0019] A method of purifying exhaust gases recited in claim 7 is characterized in placing, in exhaust gases in oxygen-excessive atmospheres, a catalyst produced by loading on a porous oxide support a noble metal composite colloid composed of a plurality of noble metals and an NO<sub>x</sub> storage component selected from alkali metals, alkaline-earth metals and rare-earth elements so as to adsorb NO<sub>x</sub> in the exhaust gases on the NO<sub>x</sub> storage component, and changing the exhaust gas atmospheres to the stoichiometric point or on the fuel-rich side so as to release the NO<sub>x</sub> from the NO<sub>x</sub> storage component and reduce the NO<sub>x</sub>.

#### 45 BRIEF DESCRIPTION OF DRAWINGS

##### [0020]

50 Figure 1 is a graph showing the relation between colloidal particle size and the number of atoms constituting a colloid.

Figure 2 is a graph showing the Pt particle size of the catalysts of reference examples and the catalyst of Conventional Example 1 in the initial stage.

Figure 3 is a graph showing the Pt particle size of the catalysts of the reference examples and the catalyst of Conventional Example 1 after a durability test.

55 Figure 4 is a graph showing the relation between the Pt particle size of the catalysts of the reference examples and Conventional Example 1 in the initial stage and those after the durability test.

Figure 5 is a graph showing 50% conversion temperatures of the catalysts of the reference examples and the catalyst of Conventional Example 1 in the initial stage.

Figure 6 is a graph showing 50% conversion temperatures of the catalysts of the reference examples and the catalyst of Conventional Example 1 after the durability test.

Figure 7 is a graph showing the relation between the initial Pt particle size and the initial 50% conversion temperatures of the catalysts of the reference examples and the catalyst of Conventional Example 1.

Figure 8 is a graph showing the relation between the Pt particle size in the initial stage and the 50% conversion temperatures after the durability test of the catalysts of the reference examples and the catalyst of Conventional Example 1.

Figure 9 is a graph showing the amounts of CO adsorbed to the catalysts of Reference Example 13 and the catalyst of Conventional Example 2 in the initial stage.

Figure 10 is a graph showing the Pt particle size of the catalyst of Reference Example 13 and the catalyst of Conventional Example 2 after a durability test.

Figure 11 is a graph showing 50% conversion temperatures of the catalyst of Reference Example 13 and the catalyst of Conventional Example 2 in the initial stage.

Figure 12 is a graph showing 50% conversion temperatures of the catalyst of Reference Example 13 and the catalyst of Conventional Example 2 after the durability test.

Figure 13 is a graph showing the relation between the amounts of Rh and the particle size of noble metal colloids of the catalysts of Reference Examples 14 to 22 in the initial stage.

Figure 14 is a graph showing the relation between the amounts of Rh and the particle size of noble metal colloids of the catalysts of Reference Examples 14 to 22 and the catalysts of Conventional Examples 3 to 11 after a durability test.

Figure 15 is a graph showing 50% conversion temperatures of the catalysts of Reference Examples 14 to 22 and the catalyst of Reference Example 4 in the initial stage.

Figure 16 is a graph showing 50% conversion temperatures of the catalysts of Reference Examples 14 to 22 and the catalyst of Reference Example 4 after the durability test.

Figure 17 is a graph showing 50% conversion temperatures of the catalysts of Conventional Examples 3 to 11 and the catalyst of Conventional Example 1 after the durability test.

Figure 18 is a schematic explanatory view of the change of colloidal particles in the production method of Reference Example 23.

Figure 19 is an explanatory view showing the structure of the catalyst of Example 1 schematically.

Figure 20 is an explanatory view showing the structure of the catalyst of Comparative Example 1 schematically.

Figure 21 is a graph showing the amounts of NO<sub>x</sub> adsorbed to the catalysts of Examples 1 to 3 and Comparative Examples 1 to 3 in the initial stage.

Figure 22 is a graph showing the amounts of NO<sub>x</sub> adsorbed to the catalysts of Examples 1 to 3 and Comparative Examples 1 to 3 after a durability test.

Figure 23 is an electromicroscopic photograph showing the particle structure of the catalyst of Example 1 in the initial stage.

Figure 24 is an electromicroscopic photograph showing the particle structure of the catalyst of Example 1 after the durability test.

Figure 25 is an electromicroscopic photograph showing the particle structure of the catalyst of Comparative Example 1.

Figure 26 is a graph showing 50% conversion temperatures of the catalysts of Examples 1 to 3 and Comparative Examples 1 to 3 in the initial stage.

Figure 27 is a graph showing 50% conversion temperatures of the catalysts of Examples 1 to 3 and Comparative Examples 1 to 3 after the durability test.

Figure 28 is a graph showing the amounts of sulfur adsorbed to the catalysts of Examples 1 to 3 and Comparative Examples 1 to 3.

Figure 29 is an explanatory view showing the micro structure of the catalyst of Example 1 schematically.

Figure 30 is an explanatory view showing the micro structure of the catalyst of Example 4.

Figure 31 is a graph showing the saturated amounts of NO<sub>x</sub> adsorbed to the catalysts of Examples 4 to 5 and Comparative Examples 4 to 7 in the initial stage.

Figure 32 is a graph showing the amounts of NO<sub>x</sub> adsorbed to the catalyst of Examples 4 to 5 and Comparative Examples 4 to 7 after fuel-rich spikes.

Figure 33 is a graph showing the saturated amounts of NO<sub>x</sub> adsorbed to the catalysts of Examples 4 to 5 and Comparative Examples 4 to 7 after a durability test.

Figure 34 is a graph showing the amounts of NO<sub>x</sub> adsorbed to the catalysts of Examples 4 to 5 and Comparative Examples 4 to 7 after fuel-rich spikes after the durability test.

Figure 35 is a graph showing 50% conversion temperatures of the catalysts of Examples 4 to 5 and Comparative Examples 4 to 7 in the initial stage.

Figure 36 is a graph showing 50% conversion temperatures of the catalysts of Examples 4 to 5 and Comparative Examples 4 to 7 after the durability test.

#### THE BEST MODES FOR CARRYING OUT THE INVENTION

[0021] In the conventional catalyst, since Pt is loaded while highly dispersed on an atomic level, grain growth is supposed to be caused by the following two mechanisms.

(1) In fuel-lean oxygen-excessive atmospheres at high temperatures, Pt is oxidized into volatile  $\text{PtO}_2$ , which leaves the original loaded positions and diffuses to be caught by other Pt atoms or Pt micro particles. Thus, grain growth is caused.

(2) For example, owing to a small affinity of Pt and  $\text{Al}_2\text{O}_3$ , Pt atoms or Pt micro particles easily move on the surface of an  $\text{Al}_2\text{O}_3$  support, repeatedly collide against and fuse with each other. Thus grain growth is caused.

[0022] In the above mechanism (1), the dislocation and diffusion of  $\text{PtO}_2$  is dependent on its vapor pressure. A smaller particle with a higher vapor pressure leaves its original position and diffuses more easily. When this particle becomes a larger particle with a lower vapor pressure by grain growth, the particle becomes stable. Thus grain growth is caused. Therefore, grain growth can be suppressed by loading beforehand Pt particles of a size which does not allow easy dislocation or diffusion.

[0023] On the other hand, in the mechanism (2), grain growth can be suppressed by increasing the affinity of Pt and  $\text{Al}_2\text{O}_3$ .

[0024] In the exhaust-gases-purifying catalysts recited in claim 2, noble metals are loaded in the state of a noble metal composite colloid. Since the noble metals are loaded as noble metal colloidal particles which are respectively assemblies of ten to several thousands of atoms,  $\text{PtO}_2$  is suppressed from dislocation or diffusion in oxygen-excessive fuel-lean atmospheres at high temperatures when compared with  $\text{PtO}_2$  in the case of using the conventional exhaust-gases-purifying catalysts in which a noble metal is loaded in the atomic state. Thus, grain growth due to the above mechanism (1) is suppressed.

[0025] Moreover, noble metals are loaded in the state of a noble metal composite colloid composed of a plurality of noble metals. Therefore, for example, when Pt and Rh or Pt and Pd are made into a composite, there is generated  $\text{Rh}_2\text{O}_3$ ,  $\text{RhO}$ ,  $\text{PdO}$ , or the like, which has a great affinity with a support formed of  $\text{Al}_2\text{O}_3$  or the like. Also the noble metal composite colloid and  $\text{Al}_2\text{O}_3$  have a high affinity with each other. Consequently, the noble metal composite colloid is suppressed from moving on the support and grain growth due to the mechanism (2) is suppressed.

[0026] The particle size of the loaded noble metal composite colloid is preferably in the range from 1 to 5 nm. Theoretically, the particle size of the colloid and the number of constituent atoms have the relation shown in Figure 1. When the particle size is from 1 to 5 nm, the number of constituent atoms is from 10 to 3000. When the particle size is smaller than 1 nm, the colloid is very close to the atomic state and grain growth due to the mechanism (1) is liable to be observed. When the particle size is greater than 5 nm, the surface area of the noble metal composite colloid decreases and the initial conversion ratio lowers. With a particle size of 1 to 5 nm, grain growth due to the mechanisms (1) and (2) can be suppressed efficiently, so the durability is improved and at the same time a high initial conversion activity can be secured owing to the large surface area of the noble metal composite colloid.

[0027] As noble metals constituting the noble metal composite colloid, it is possible to employ iridium (Ir), silver (Ag) and so on besides Pt, Rh and Pd. Two or more kinds of these noble metals can be selected for use. It is desirable to employ at least Pt, which has an especially high catalytic activity. It is desirable to employ Pt and Rh in combination. Because the grain growth of Rh in fuel-lean atmospheres is remarkably small when compared with Pt, the existence of Rh improves the durability of the three-way catalytic activity. In addition, because Rh is loaded in separation from an  $\text{NO}_x$  storage component on a micro scale, the poor affinity of Rh and the  $\text{NO}_x$  storage component does not become a problem, and the performance of the  $\text{NO}_x$  storage component and Rh is prevented from degrading.

[0028] Furthermore, when Pt and Rh are employed in combination, hydrogen, which has a high reducing power, is generated from HC and  $\text{H}_2\text{O}$  in exhaust gases because of Rh, and this hydrogen highly contributes to reduction of  $\text{NO}_x$  and dislocation of  $\text{SO}_x$ . Consequently, when compared with the conventional catalyst, the amount of  $\text{NO}_x$  reduced after fuel-rich spikes becomes high and at the same time sulfur poisoning of the  $\text{NO}_x$  storage component is extremely small.

[0029] In the catalysts recited in claim 2, the amount of a noble metal composite colloid loaded can be, for example, in the range from 0.1 to 20 % by weight. When the amount is less than 0.1 % by weight, the conversion ratio is low from the initial stage. The amount of more than 20 % by weight is not suitable for industrial use, because of saturation of catalyst efficiency and high production costs. The ratio of the plurality of noble metals which constitute a noble metal composite colloid is not particularly limited, but there are sometimes optimum ratios depending on the kind of noble metals. For example, when a noble metal composite colloid is composed of Pt and Rh, it is desirable that the noble

metal composite colloid contains 10 to 80 mol% Rh. Within this range, the conversion activity in the initial stage and after the durability test is particularly excellent.

**[0030]** Examples of the porous oxide support include alumina ( $\text{Al}_2\text{O}_3$ ), silica ( $\text{SiO}_2$ ), titania ( $\text{TiO}_2$ ), zirconia ( $\text{ZrO}_2$ ), silica-alumina, and zeolite.

**[0031]** As an  $\text{NO}_x$  storage element constituting the  $\text{NO}_x$  storage component, it is possible to use at least one element selected from alkali metals, alkaline-earth metals and rare-earth elements. Examples of alkali metals are lithium (Li), sodium (Na), potassium (K) and cesium (Cs). Alkaline-earth metals are the elements of Group IIA in the periodic table and include, for example, magnesium (Mg), calcium (Ca), strontium (Sr) and barium (Ba). Examples of rare-earth elements are lanthanum (La), cerium (Ce), praseodymium (Pr).

**[0032]** The desirable amount of this  $\text{NO}_x$  storage component to be loaded is in the range from 0.05 to 0.5 mol with respect to 120g of the porous oxide support. When the amount is less than this range, the  $\text{NO}_x$  conversion ability can hardly be exhibited. When the amount exceeds this range, not only the effect of the  $\text{NO}_x$  storage component is saturated but also the amount of noble metals to be loaded decreases and the conversion activity deteriorates.

**[0033]** In loading the  $\text{NO}_x$  storage component on the porous oxide support, a similar method to the conventional method can be employed which comprises the steps of impregnating a porous oxide support with a solution of a soluble salt or complex of the above  $\text{NO}_x$  storage elements, and drying and calcining the impregnated support.

**[0034]** By the way, the porous support has a great number of micro pores, and HC, etc., in exhaust gases are often adsorbed in the micro pores. For example, since zeolite has micro pores of a size on the angstrom order, which is approximately equal to the order of the molecule diameter of HC, zeolite is even used as a HC adsorbent. Therefore, it is desirable to oxidize HC adsorbed in the micro pores efficiently, or use the adsorbed HC to reduce  $\text{NO}_x$  into innocuous entities.

**[0035]** However, because of the relatively large particle size, the noble metal composite colloid according to the present invention suffers from a drawback in that it is difficult to load the noble metal composite colloid in the relatively small diameter micro pores of the porous oxide support and that HC adsorbed in the micro pores are used at a low efficiency. Besides, owing to its adsorption characteristics the  $\text{NO}_x$  storage component is loaded both on the surface and in the micro pores of the porous oxide support, but there is also a problem that the  $\text{NO}_x$  storage component loaded in the micro pores is utilized at a low efficiency when no noble metal exists in the micro pores.

**[0036]** Therefore, in the exhaust-gases-purifying catalyst recited in claim 3, a noble metal composite colloid is loaded on the surface of the porous oxide support, and a noble metal in the atomic state is loaded in the micro pores of the porous oxide support. Owing to this arrangement, HC adsorbed in the micro pores can be oxidized efficiently and the three-way activity is enhanced.

**[0037]** In the exhaust-gases-purifying catalyst recited in claim 4, a noble metal composite colloid and an  $\text{NO}_x$  storage component are loaded on the surface of a porous oxide support, and a noble metal in the atomic state and an  $\text{NO}_x$  storage component are loaded in the micro pores of the porous oxide support. Owing to this arrangement, the  $\text{NO}_x$  storage component loaded in the micro pores is improved in utilization efficiency and the  $\text{NO}_x$  conversion activity is enhanced.

**[0038]** In the exhaust-gases-purifying catalysts recited in claim 3 and claim 4, it is preferable that the amount of the noble metal composite colloid loaded and the amount of a noble metal loaded in the atomic state have a ratio by weight of about 1 to 1. When the noble metal in the atomic state is loaded beyond this ratio, the noble metal becomes to be loaded not only in the micro pores but also on the surface of the porous oxide support, which results in easy grain growth. On the other hand, when the noble metal in the atomic state is loaded under this ratio, HC adsorbed in the micro pores are hard to be oxidized, which results in a decrease in the utilization efficiency of the  $\text{NO}_x$  storage component loaded in the micro pores.

**[0039]** Several methods can be employed for producing a noble metal composite colloid and loading the colloid on a porous oxide support: a method of utilizing electrostatic adsorption, a method of utilizing high polymer chain adsorption to the support, the method of using a surfactant-protected noble metal composite colloid recited in claim 6, etc.

**[0040]** For instance, in the method of utilizing high polymer chain adsorption to the support, first a plurality of water-soluble noble metal compounds and alcohol are mixed in an aqueous solution of a water-soluble high polymer such as polyvinyl pyrrolidone, polyvinyl alcohol and heated, thereby forming a polymer-protected noble metal composite colloid. This method is called a polymer protection method. Then porous support powder formed of such an oxide as alumina is dispersed in this aqueous solution of the polymer-protected noble metal composite colloid, and then dried and calcined, thereby producing noble metal composite colloid-loaded catalyst powder. A catalyst for purifying exhaust gases can be produced by coating this catalyst powder on a honeycomb supporting base material, etc.

**[0041]** However, in the above production method, the polymer chains of the polymeric material serving as a protective agent lie extensively in an aqueous solution of a polymer-protected noble metal composite colloid and accordingly colloidal particles in the aqueous solution have a large radius (fluid radius). So, clearly this production method has a defect in that the colloidal particles are prevented from diffusing into relatively large micro pores of the porous oxide support, which results in poor adsorption to the support.

[0042] In view of this, the noble metal composite colloid is loaded preferably by bringing the porous oxide support in contact with a surfactant-protected noble metal composite colloidal solution. The surfactant-protected noble metal composite colloid has a smaller colloidal particle fluid radius, because the molecule length of the surfactant which acts as a protective agent in the surfactant-protected noble metal composite colloid is smaller than that of the polymeric material which acts as a protective agent in the polymer-protected noble metal composite colloid. Therefore the colloid adsorption performance to the support improves. Besides, since electrostatic characteristics of the colloidal particle surface can be controlled freely by pH control, selective adsorption to the support can be improved. In the case of using a plurality of porous oxide supports, setting of appropriate conditions enables plural kinds of colloidal particles to be loaded on plural kinds of supports respectively in separation.

[0043] In this exhaust-gases-purifying catalyst production method, first in a separation step, a noble metal composite colloid is taken out of a polymer-protected noble metal composite colloid. This separation step is carried out simply, for example, by removing a polymeric protective agent from the polymer-protected noble metal composite colloid. It is possible to use a ligand substitution method, a method of hydrolyzing the polymeric protective agent, etc. for this purpose.

[0044] The noble metal composite colloid obtained in the separation step is dispersed in water by using a surfactant, thereby formed into a surfactant-protected noble metal composite colloidal solution. The surfactant to be employed can be anionic, cationic, amphoteric or nonionic. It is particularly preferable to use such a surfactant which tends to form a micell in an aqueous solution as sodium lauryl sulfate, lauryl trimethyl ammonium chloride, polyethylene glycol lauryl ether and  $\beta$ -N-lauryl amino propionic acid.

[0045] Then a porous oxide support can be brought in contact with the surfactant-protected noble metal composite colloidal solution and dried and calcined to obtain catalyst powder in which a noble metal composite colloid is loaded on the porous oxide support. This catalyst powder can be coated on a honeycomb supporting base material, etc. formed of a heat-resistant oxide such as cordierite or a metal to obtain a catalyst for purifying exhaust gases.

[0046] Besides, the exhaust-gases-purifying catalyst recited in claim 2 can be produced by loading an  $\text{NO}_x$  storage component on the porous oxide support by the aforementioned method, after this exhaust-gases-purifying catalyst production method is carried out, or before or after the porous oxide support is brought in contact with the surfactant-protected noble metal composite colloidal solution.

[0047] In the case of producing the exhaust-gases-purifying catalyst recited in claim 4; it is necessary to load an atomic-state noble metal only in the micro pores of the porous oxide support. This is because it becomes difficult to suppress grain growth of the noble metal when the noble metal in the atomic state is loaded on the surface of the support. However, if a noble metal is loaded by using an aqueous solution of a noble metal compound just as in the general conventional method, there arises a problem that the noble metal is loaded not only in the micro pores but also on the surface of the support.

[0048] Therefore, in the production method recited in claim 6, a noble metal in the atomic state is loaded by bringing the porous oxide support in contact with a solution of pyromellitic acid and a noble metal compound in water. Because of its relatively large molecular size, pyromellitic acid is difficult to enter into the relatively small diameter micro pores of the porous oxide support. In addition, since the hydroxyl group of the porous oxide support is masked with pyromellitic acid, it is difficult to load a noble metal by chemical adsorption. Therefore, when the porous oxide support is brought in contact with a solution of pyromellitic acid and a noble metal compound in water, the hydroxyl group on the support surface is masked with the pyromellitic acid but the hydroxyl group in the micro pores is not masked, i.e., is revealed, so the noble metal is loaded in the micro pores by chemical adsorption according to priority. Thus, the noble metal in the atomic state can be loaded only in the micro pores.

[0049] The noble metal colloid-loading step and the atomic-state noble metal-loading step recited in claim 6 can be carried out separately or simultaneously as described in the preferred embodiments.

[0050] In the exhaust-gases-purifying method recited in claim 7, the catalyst recited in claim 2 is placed in exhaust gases in oxygen-excessive fuel-lean atmospheres so that the  $\text{NO}_x$  storage component adsorbs  $\text{NO}_x$  in the exhaust gases. Then the exhaust gas atmospheres can be at the stoichiometric point or on the fuel-rich side so that the  $\text{NO}_x$  storage component releases the  $\text{NO}_x$ , and the released  $\text{NO}_x$  are reduced into innocuous entities by HC and CO in the exhaust gases or  $\text{H}_2$  generated by Rh.

[0051] According to this method of purifying exhaust gases, grain growth of noble metals is suppressed and as a result the amount of  $\text{NO}_x$  stored can be prevented from decreasing after a durability test, etc. Also since grain growth of noble metals is suppressed, the  $\text{NO}_x$  storage component is prevented from suffering from sulfur poisoning. Therefore, the durability of the  $\text{NO}_x$  conversion ability is improved.

[0052] It must be noted that in this method of purifying exhaust gases, the conditions of changing the exhaust gas atmospheres from the fuel-lean side to the stoichiometric point or the fuel-rich side are not particularly limited and optimal conditions for use can be employed.

## EP 1 043 065 B1

(Preferred Embodiments)

**[0053]** Hereinafter, the present invention will be explained concretely by reference examples, examples and comparative examples.

(Reference Example 1)

**[0054]** 0.6566g of  $\text{PtCl}_4 \cdot 5\text{H}_2\text{O}$  and 7.39g of sodium dodecyl sulfate were mixed in 500g of water and stirred so as to prepare a uniform aqueous solution. Then, 10g of citrate dihydrate was added to this aqueous solution and the mixture was treated at reflux at 100 °C for two hours, thereby obtaining a Pt colloidal solution. 24g of  $\gamma\text{-Al}_2\text{O}_3$  powder was introduced into this colloidal solution. The mixture was stirred for 15 minutes and then filtered. After dried at 110 °C for two hours, this material was calcined at 450 °C for two hours, thereby obtaining a Pt colloid-loaded catalyst. The amount of Pt loaded was  $6.4 \times 10^{-5}$  mol with respect to 1 g of  $\gamma\text{-Al}_2\text{O}_3$  powder.

(Reference Example 2)

**[0055]** 0.6566g of  $\text{PtCl}_4 \cdot 5\text{H}_2\text{O}$  and 4.27g of sodium laurate were mixed in 500g of water and stirred to prepare a uniform aqueous solution. 10g of citrate dihydrate was added to this aqueous solution. This mixture was treated at reflux at 100 °C for two hours, thereby obtaining a Pt colloidal solution. 24g of  $\gamma\text{-Al}_2\text{O}_3$  powder was introduced into this colloidal solution and nitric acid was added to this solution so as to adjust pH to 4. The solution was stirred for 15 minutes and then filtered. After dried at 110 °C for two hours, this material was calcined at 450 °C for two hours, thereby obtaining a Pt colloid-loaded catalyst. The amount of Pt loaded was  $6.4 \times 10^{-5}$  mol with respect to 1 g of  $\gamma\text{-Al}_2\text{O}_3$  powder. The reason why the pH was adjusted to 4 was to remove counter ions which electrostatically shield the colloidal surface and increase the electrostatic charge on the colloidal surface.

(Reference Example 3)

**[0056]** 0.6566g of  $\text{PtCl}_4 \cdot 5\text{H}_2\text{O}$  and 0.89g of polyvinyl pyrrolidone with a number average molecular weight of 25,000 were mixed in 400g of water and stirred to prepare a uniform aqueous solution. 100g of ethanol was added to this aqueous solution, and this mixture was treated at reflux at 90 °C for two hours, thereby obtaining a Pt colloidal solution. 24g of  $\gamma\text{-Al}_2\text{O}_3$  powder was introduced into this colloidal solution and the mixture was concentrated and dried to obtain solids. After dried at 110 °C for two hours, this material was calcined at 450 °C for two hours, thereby obtaining a Pt colloid-loaded catalyst. The amount of Pt loaded was  $6.4 \times 10^{-5}$  mol with respect to 1g of  $\gamma\text{-Al}_2\text{O}_3$  powder.

(Reference Example 4)

**[0057]** 0.6566g of  $\text{PtCl}_4 \cdot 5\text{H}_2\text{O}$  and 0.89g of polyvinyl pyrrolidone with a number average molecular weight of 25,000 were mixed in 400g of water and stirred to prepare a uniform aqueous solution. 100g of ethanol was added to this aqueous solution, and this mixture was treated at reflux at 90 °C for two hours, thereby obtaining a Pt colloidal solution. This colloidal solution was concentrated by using a rotary evaporator, thereby obtaining a solution at a Pt concentration of 5 % by weight.

**[0058]** On the other hand, 24g of  $\gamma\text{-Al}_2\text{O}_3$  powder was dispersed in 300g of water and then 6g of the aforementioned solution was added and the mixture was stirred for 30 minutes and then filtered. After dried at 110 °C for two hours, this material was calcined at 450 °C for two hours, thereby obtaining a Pt colloid-loaded catalyst. The amount of Pt loaded was  $6.4 \times 10^{-5}$  mol with respect to 1g of  $\gamma\text{-Al}_2\text{O}_3$  powder.

(Reference Example 5)

**[0059]** 0.6566g of  $\text{PtCl}_4 \cdot 5\text{H}_2\text{O}$  and 0.89g of polyvinyl pyrrolidone with a number average molecular weight of 25,000 were mixed in 400g of water and the mixture was stirred to prepare a uniform aqueous solution. 100g of ethanol was added to this aqueous solution and, this mixture was treated at reflux at 90 °C for two hours, thereby obtaining a Pt colloidal solution. This colloidal solution was concentrated by using a rotary evaporator into black paste. Then the paste was dried under vacuum, thereby obtaining Pt colloid powder. This Pt colloid powder was dispersed in water to prepare a Pt colloidal solution at a Pt concentration of 5% by weight.

**[0060]** On the other hand, 24g of  $\gamma\text{-Al}_2\text{O}_3$  powder was dispersed in 300g of water and 6g of the above Pt colloidal solution was added and stirred for 30 minutes and then filtered. After dried at 110 °C for two hours, this material was calcined at 450 °C for two hours, thereby obtaining a Pt colloid-loaded catalyst. The amount of Pt loaded was  $6.4 \times 10^{-5}$  mol with respect to 1g of  $\gamma\text{-Al}_2\text{O}_3$  powder.



## EP 1 043 065 B1

(Reference Example 6)

[0061] 0.6566g of  $\text{PtCl}_4 \cdot (5\text{H}_2\text{O})$  and 0.89g of polyvinyl pyrrolidone with a number average molecular weight of 25,000 were mixed in 400g of water and the mixture was stirred to prepare a uniform aqueous solution. 100g of ethanol was added to this aqueous solution and, this mixture was treated at reflux at 90 °C for two hours, thereby obtaining a Pt colloidal solution. These steps are the same as those of Reference Example 4.

[0062] Next, this colloidal solution was cooled to 20 °C, and 0.4236g of  $\text{PtCl}_4 \cdot (5\text{H}_2\text{O})$  was added. After stirred for one hour, this solution was treated at reflux at 90 °C for two hours. This colloidal solution was concentrated by using a rotary evaporator so as to prepare a solution at a Pt concentration of 5 % by weight.

[0063] On the other hand, 24g of  $\gamma\text{-Al}_2\text{O}_3$  powder was dispersed in 300g of water and 6 g of the above solution was added and stirred for 30 minutes and filtered. After dried at 110 °C for two hours, this material was calcined at 450 °C for two hours, thereby obtaining a Pt colloid-loaded catalyst. The amount of Pt loaded was  $6.4 \times 10^{-5}$  mol with respect to 1g of  $\gamma\text{-Al}_2\text{O}_3$  powder.

(Reference Example 7)

[0064] A catalyst was produced in a similar method to that of Reference Example 6 except that  $\text{PtCl}_4 \cdot (5\text{H}_2\text{O})$  for the second addition was in an amount of 0.5767g instead of 0.4236g. The amount of Pt loaded was  $6.4 \times 10^{-5}$  mol with respect to 1g of  $\gamma\text{-Al}_2\text{O}_3$  powder.

(Reference Example 8)

[0065] A catalyst was produced in a similar method to that of Reference Example 6 except that  $\text{PtCl}_4 \cdot (5\text{H}_2\text{O})$  for the second addition was in an amount of 0.7512g instead of 0.4236g. The amount of Pt loaded was  $6.4 \times 10^{-5}$  mol with respect to  $\gamma\text{-Al}_2\text{O}_3$  powder.

(Reference Example 9)

[0066] A catalyst was produced in a similar method to that of Reference Example 6 except that  $\text{PtCl}_4 \cdot (5\text{H}_2\text{O})$  for the second addition was in an amount of 0.9501g instead of 0.4236g. The amount of Pt loaded was  $6.4 \times 10^{-5}$  mol with respect to 1 g of  $\gamma\text{-Al}_2\text{O}_3$  powder.

(Reference Example 10)

[0067] A catalyst was produced in a similar method to that of Reference Example 6 except that  $\text{PtCl}_4 \cdot (5\text{H}_2\text{O})$  for the second addition was in an amount of 1.1723g instead of 0.4236g. The amount of Pt loaded was  $6.4 \times 10^{-5}$  mol with respect to 1g of  $\gamma\text{-Al}_2\text{O}_3$  powder.

(Reference Example 11)

[0068] A catalyst was produced in a similar method to that of Reference Example 3 except that the amount of polyvinyl pyrrolidone was 3.39g instead of 0.89g. The amount of Pt loaded was  $6.4 \times 10^{-5}$  mol with respect to 1g of  $\gamma\text{-Al}_2\text{O}_3$  powder.

(Reference Example 12)

[0069] A catalyst was produced in a similar method to that of Reference Example 3 except that the amount of polyvinyl pyrrolidone was 9.05g instead of 0.89g. The amount of Pt loaded was  $6.4 \times 10^{-5}$  mol with respect to 1g of  $\gamma\text{-Al}_2\text{O}_3$  powder.

(Conventional Example 1)

[0070] 24g of  $\gamma\text{-Al}_2\text{O}_3$  powder was introduced into 500g of a nitric acid solution including a platinum dinitrodiamine complex (including 0.25g of Pt) and stirred for 15 minutes and then filtered. After dried at 110 °C for two hours, the material was calcined at 450 °C for two hours, thereby obtaining a catalyst of Conventional Example 1. The amount of Pt loaded was  $6.4 \times 10^{-5}$  mol with respect to 1g of  $\gamma\text{-Al}_2\text{O}_3$  powder.

<Experiment 1>

[0071] The Pt particle size of the catalysts of the above Reference Examples 1 to 12 and Conventional Example 1

# EP 1 043 065 B1

were respectively measured by the CO pulse method. The results are presented in Figure 2. Besides, a durability test in which each catalyst was calcined at 800 °C for 10 hours in the air was carried out. The measurements of the Pt particle size after the durability test by the X-ray diffraction method are shown in Figure 3. Figure 4 shows the relation between the Pt particle sizes in the initial stage and those after the durability test, which are plotted from the respective results.

## <Experiment 2>

**[0072]** The catalysts of the above Reference Examples 1 to 12 and Conventional Example 1 were respectively placed in laboratory reactors and a model exhaust gas with the composition shown in Table 1 was introduced at a gas space velocity of 20,000 hr<sup>-1</sup>. Then the catalyst bed temperature was varied in the range from 25 to 600 °C, and the catalyst bed temperatures at the 50% conversion of HC (C<sub>3</sub>H<sub>6</sub>), CO and NO were measured. The results are shown in Figure 5. A durability test was carried out in the same way as in Experiment 1 and the 50% conversion temperatures of the respective catalysts after the durability test were measured, and the results are presented in Figure 6. Furthermore the relations between the 50% conversion temperatures in the initial stage or those after the durability test and the initial Pt particle size are respectively shown in Figures 7 and 8.

[Table 1]

| GAS   | C <sub>3</sub> H <sub>6</sub><br>(ppm) | CO<br>(ppm) | NO<br>(ppm) | H <sub>2</sub><br>(ppm) | O <sub>2</sub><br>(%) | CO <sub>2</sub><br>(%) | H <sub>2</sub> O<br>(%) | N <sub>2</sub> |
|-------|--|-------------|-------------|-------------------------|-----------------------|------------------------|-------------------------|----------------|
| COMP. | 7200                                   | 1200        | 2400        | 400                     | 0.50                  | 14.4                   | 3                       | balance        |

## <Evaluation>

**[0073]** It is appreciated from Figures 2 to 4 that the respective catalysts of the reference examples had larger initial Pt particle sizes than the initial Pt particle size (less than 1 nm) of Conventional Example 1 but kept to have smaller Pt particle sizes than that of Conventional Example 1 after the durability test. It is clear from Figure 6 that the respective catalysts of the reference examples had remarkably better conversion abilities than that of Conventional Example 1 after the durability test. That is to say, in the respective catalysts of the reference examples, Pt grain growth was suppressed when compared with that of Conventional Example 1. This is apparently an effect of loading Pt as a colloid of 1 nm or more in particle size.

**[0074]** However, it is also apparent from Figure 7 that the initial particle size of the Pt colloid is desirably in the range from 1 to 5 nm because the initial 50% conversion temperatures exceeded 300 °C when the initial Pt particle size was over 5 nm.

**[0075]** In view of the above results, the particle size of the noble metal composite colloid in the initial stage was controlled to be about 3 nm in the following reference examples.

### (Reference Example 13)

**[0076]** 0.591g of PtCl<sub>4</sub> (5H<sub>2</sub>O), 0.027g of PdCl<sub>2</sub> and 0.89g of polyvinyl pyrrolidone with a number average molecular weight of 25,000 were mixed in 400g of water and the mixture was stirred to prepare a uniform aqueous solution. 100g of ethanol was added to this aqueous solution and the mixture was treated at reflux at 90 °C for two hours, thereby obtaining a Pt-Pd composite colloidal solution (Pt: 90mol%, Pd: 10mol%). This colloidal solution was concentrated by using a rotary evaporator so as to obtain a solution at the total noble metal concentration of 2.73 % by weight (Pt: 2.57% by weight, Pd: 0.16% by weight).

**[0077]** On the other hand, 24g of γ-Al<sub>2</sub>O<sub>3</sub> powder was dispersed in 300g of water. Then 10.5g of the above solution was added to this and stirred for 30 minutes and filtered. After dried at 110 °C for two hours, this material was calcined at 450 °C for two hours, thereby obtaining a Pt-Pd composite colloid-loaded catalyst. The amounts of noble metals loaded were 6.4 x 10<sup>-5</sup> mol in total of Pt and Pd with respect to 1g of γ-Al<sub>2</sub>O<sub>3</sub> powder.

### (Reference Example 14)

**[0078]** 0.591g of PtCl<sub>4</sub> (5H<sub>2</sub>O), 0.0405g of RhCl<sub>3</sub> (3H<sub>2</sub>O) and 0.89g of polyvinyl pyrrolidone with a number average molecular weight of 25,000 were mixed in 400g of water and stirred to prepare a uniform aqueous solution. 100g of ethanol was added to this aqueous solution and the mixture was treated at reflux at 90 °C for two hours, thereby obtaining a Pt-Rh composite colloidal solution (Pt: 90mol%, Rh: 10mol%). This colloidal solution was concentrated by using a rotary evaporator so as to obtain a solution at the total noble metal concentration of 2.17% by weight (Pt: 2.05%

by weight, Rh: 0.12% by weight).

[0079] On the other hand, 24g of  $\gamma\text{-Al}_2\text{O}_3$  powder was dispersed in 300g of water and 13.17g of the above solution was added to this and stirred for 30 minutes and filtered. After dried at 110°C for two hours, this material was calcined at 450 °C for two hours, thereby obtaining a Pt-Rh composite colloid-loaded catalyst. The amounts of noble metals loaded were  $6.4 \times 10^{-5}$  mol in total of Pt and Rh with respect to 1g of  $\gamma\text{-Al}_2\text{O}_3$  powder.

(Reference Example 15)

[0080] A Pt-Rh composite colloidal solution (Pt: 80mol%, Rh: 20mol%) was obtained in the same way as that of Reference Example 14 except that the amounts of  $\text{PtCl}_4 (5\text{H}_2\text{O})$  and  $\text{RhCl}_3 (3\text{H}_2\text{O})$  added were different from those of Reference Example 14. This colloidal solution was concentrated by using a rotary evaporator in the same way as in Reference Example 14, and the colloid was loaded in the same way as in Reference Example 14, thereby obtaining a Pt-Rh composite colloid-loaded catalyst. The amounts of noble metals loaded were  $6.4 \times 10^{-5}$  mol in total of Pt and Rh with respect to 1g of  $\gamma\text{-Al}_2\text{O}_3$  powder.

(Reference Example 16)

[0081] A Pt-Rh composite colloidal solution (Pt: 70mol%, Rh: 30mol%) was obtained in the same way as that of Reference Example 14 except that the amounts of  $\text{PtCl}_4 (5\text{H}_2\text{O})$  and  $\text{RhCl}_3 (3\text{H}_2\text{O})$  added were different from those of Reference Example 14. This colloidal solution was concentrated by using a rotary evaporator in the same way as in Reference Example 14, and the colloid was loaded in the same way as in Reference Example 14, thereby obtaining a Pt-Rh composite colloid-loaded catalyst. The amounts of noble metals loaded were  $6.4 \times 10^{-5}$  mol in total of Pt and Rh with respect to 1g of  $\gamma\text{-Al}_2\text{O}_3$  powder.

(Reference Example 17)

[0082] A Pt-Rh composite colloidal solution (Pt: 60mol%, Rh: 40mol%) was obtained in the same way as that of Reference Example 14 except that the amounts of  $\text{PtCl}_4 (5\text{H}_2\text{O})$  and  $\text{RhCl}_3 (3\text{H}_2\text{O})$  added were different from those of Reference Example 14. This colloidal solution was concentrated by using a rotary evaporator in the same way as in Reference Example 14, and the colloid was loaded in the same way as in Reference Example 14, thereby obtaining a Pt-Rh composite colloid-loaded catalyst. The amounts of noble metals loaded were  $6.4 \times 10^{-5}$  mol in total of Pt and Rh with respect to 1g of  $\gamma\text{-Al}_2\text{O}_3$  powder.

(Reference Example 18)

[0083] A Pt-Rh composite colloidal solution (Pt: 50mol%, Rh: 50mol%) was obtained in the same way as that of Reference Example 14, except that the amounts of  $\text{PtCl}_4 (5\text{H}_2\text{O})$  and  $\text{RhCl}_3 (3\text{H}_2\text{O})$  added were different from those of Reference Example 14. This colloidal solution was concentrated by using a rotary evaporator in the same way as in Reference Example 14, and the colloid was loaded in the same way as in Reference Example 14, thereby obtaining a Pt-Rh composite colloid-loaded catalyst. The amounts of noble metals loaded were  $6.4 \times 10^{-5}$  mol in total of Pt and Rh with respect to 1g of  $\gamma\text{-Al}_2\text{O}_3$  powder.

(Reference Example 19)

[0084] A Pt-Rh composite colloidal solution (Pt: 40mol%, Rh: 60mol%) was obtained in the same way as that of Reference Example 14, except that the amounts of  $\text{PtCl}_4 (5\text{H}_2\text{O})$  and  $\text{RhCl}_3 (3\text{H}_2\text{O})$  added were different from those of Reference Example 14. This colloidal solution was concentrated by using a rotary evaporator in the same way as in Reference Example 14, and the colloid was loaded in the same way as in Reference Example 14, thereby obtaining a Pt-Rh composite colloid-loaded catalyst. The amounts of noble metals loaded were  $6.4 \times 10^{-5}$  mol in total of Pt and Rh with respect to 1g of  $\gamma\text{-Al}_2\text{O}_3$  powder.

(Reference Example 20)

[0085] A Pt-Rh composite colloidal solution (Pt: 30mol%, Rh: 70mol%) was obtained in the same way as that of Reference Example 14, except that the amounts of  $\text{PtCl}_4 (5\text{H}_2\text{O})$  and  $\text{RhCl}_3 (3\text{H}_2\text{O})$  added were different from those of Reference Example 14. This colloidal solution was concentrated by using a rotary evaporator in the same way as in Reference Example 14, and the colloid was loaded in the same way as in Reference Example 14, thereby obtaining a Pt-Rh composite colloid-loaded catalyst. The amounts of noble metals loaded were  $6.4 \times 10^{-5}$  mol with respect to 1g

of  $\gamma\text{-Al}_2\text{O}_3$  powder.

(Reference Example 21)

[0086] A Pt-Rh composite colloidal solution (Pt: 20mol%, Rh: 80mol%) was obtained in the same way as that of Reference Example 14, except that the amounts of  $\text{PtCl}_4 \cdot (5\text{H}_2\text{O})$  and  $\text{RhCl}_3 \cdot (3\text{H}_2\text{O})$  added were different from those of Reference Example 14. This colloidal solution was concentrated by using a rotary evaporator in the same way as in Reference Example 14 and the colloid was loaded in the same way as in Reference Example 14, thereby obtaining a Pt-Rh composite colloid-loaded catalyst. The amounts of noble metals loaded were  $6.4 \times 10^{-5}$  mol with respect to 1g of  $\gamma\text{-Al}_2\text{O}_3$  powder.

(Reference Example 22)

[0087] A Pt-Rh composite colloidal solution (Pt: 10mol%, Rh: 90mol%) was obtained in the same way as that of Reference Example 14, except that the amounts of  $\text{PtCl}_4 \cdot (5\text{H}_2\text{O})$  and  $\text{RhCl}_3 \cdot (3\text{H}_2\text{O})$  added were different from those of Reference Example 14. This colloidal solution was concentrated by using a rotary evaporator in the same way as in Reference Example 14 and the colloid was loaded in the same way as in Reference Example 14, thereby obtaining a Pt-Rh composite colloid-loaded catalyst. The amounts of noble metals loaded were  $6.4 \times 10^{-5}$  mol in total of Pt and Rh with respect to 1g of  $\gamma\text{-Al}_2\text{O}_3$  powder.

(Conventional Example 2)

[0088] 24g of  $\gamma\text{-Al}_2\text{O}_3$  powder was introduced into 500g of a nitric acid solution including platinum dinitrodiamine complex and palladium nitrate (Pt: 0.27g (90mol%), Pd: 0.164g (10 mol%)) and the mixture was stirred for fifteen minutes and filtered. After dried at 110 °C for two hours, this material was calcined at 450 °C for two hours, thereby obtaining a catalyst of Conventional Example 2. The amounts of Pt and Pd loaded were the same as those of Reference Example 13.

(Conventional Examples 3 to 11)

[0089] 500g of a nitric acid solution including platinum dinitrodiamine complex and rhodium nitrate was prepared so that the total mole of Pt and Rh was 0.00154mol and the molar ratios of Pt and Rh in the respective comparative examples were those shown in Table 2. Then 24g of  $\gamma\text{-Al}_2\text{O}_3$  powder was introduced therein. The mixtures were stirred for fifteen minutes and filtered. After dried at 110 °C for two hours, these materials were calcined at 450 °C for two hours, thereby obtaining catalysts of Comparative Examples 2 to 10. The amounts of Pt and Rh loaded were the same as those of the catalysts of Reference Examples 14 to 22, i.e.,  $6.4 \times 10^{-5}$  mol in total of Pt and Rh with respect to 1g of  $\gamma\text{-Al}_2\text{O}_3$  powder.

[Table 2]

|                     |    | Pt     | Rh     |
|---------------------|----|--------|--------|
| Comparative Example | 3  | 10mol% | 90mol% |
|                     | 4  | 20mol% | 80mol% |
|                     | 5  | 30mol% | 70mol% |
|                     | 6  | 40mol% | 60mol% |
|                     | 7  | 50mol% | 50mol% |
|                     | 8  | 60mol% | 40mol% |
|                     | 9  | 70mol% | 30mol% |
|                     | 10 | 80mol% | 20mol% |
|                     | 11 | 90mol% | 10mol% |

<Experiment 3>

[0090] The dispersion degree of the noble metals in the catalysts of Reference Example 13 and Conventional Ex-

ample 2 were respectively measured by the CO pulse method, and the results are presented in Figure 9. These respective catalysts were subjected to a durability test in the same way as in Experiment 1. Figure 10 shows the particle size of the noble metals after the durability test, measured by the X-ray diffraction method. The 50% conversion temperatures of these catalysts in the initial stage and after the durability test were measured respectively and the results are shown in Figures 11 and 12.

#### <Evaluation>

[0091] It is apparent from Figure 9 that the catalyst of Reference Example 13 in the initial stage had a smaller amount of CO adsorbed and a lower dispersion degree of noble metal particles, that is to say, a larger noble metal particle size, when compared with the catalyst of Conventional Example 2 in the initial stage. When the catalysts of Reference Example 13 and Conventional Example 2 in the initial stage were analyzed by the X-ray diffraction method, the catalyst of Reference Example 13 had a noble metal particle size of 3.2nm and on the other hand, it was difficult to measure the noble metal particle size of Conventional Example 2 because the noble metals were loaded in the atomic state.

[0092] Figure 10 demonstrates that after the durability test the catalyst of Reference Example 13 had a smaller noble metal particle size than the catalyst of Conventional Example 2 and that the grain growth of noble metals by the durability test was suppressed in the catalyst of Reference Example 13.

[0093] It is also seen from Figures 11 and 12 that the catalyst of Reference Example 13 had a remarkably smaller decrease in the conversion ability after the durability test than the catalyst of Conventional Example 2, and that the catalyst of Reference Example 13 exhibited a superb conversion ability in the initial stage. This is supposed to be an effect of loading the noble metals as a composite noble metal colloid.

#### <Experiment 4>

[0094] The noble metal particle size of the catalysts of Reference Examples 14 to 22 in the initial stage were measured by the X-ray diffraction method. The results are summarized in Figure 13 with the mol% of Rh on the axis of abscissas. The catalysts of Reference Examples 14 to 22 and the catalysts of Conventional Examples 3 to 11 were subjected to a durability test in the same way as in Experiment 1, and the noble metal particle size of the respective catalysts after the durability test were measured by the X-ray diffraction method. The results are shown in Figure 14.

[0095] The 50% conversion temperatures of the catalysts of Reference Examples 14 to 22 in the initial stage and after the durability test and the 50% conversion temperatures of the catalysts of Conventional Examples 3 to 11 after the durability test were measured respectively in the same way as in Experiment 2. The results are respectively presented in Figures 15 to 17. It should be noted that Figure 15 also shows the result of Reference Example 4 on which only the Pt colloid was loaded, and that Figure 17 also shows the result of Conventional Example 1 on which only Pt was loaded.

#### <Evaluation>

[0096] As apparent from Figure 13, the initial noble metal particle size of the catalysts of Reference Examples 14 to 22 were constantly about 3 nm regardless of the amount of Rh loaded. On the other hand, the initial noble metal particle sizes of Conventional Examples 3 to 11 were too small to be measured by the X-ray diffraction method and the noble metals were loaded in the atomic state.

[0097] As evident from Figure 14, the catalysts of Reference Examples 14 to 22 had smaller noble metal particle size after the durability test than the catalysts of Conventional Examples 3 to 11; that is to say, grain growth of noble metals were suppressed and the effect of Rh was gradually stronger as the amount of Rh loaded was larger. As seen from the comparison of Figures 16 and 17, the catalysts of Reference Examples 14 to 22 had superior conversion ability after the durability test than those of Conventional Examples 3 to 11. This is supposed to be the effect of the suppression of the noble metals grain growth.

[0098] On the other hand, the comparison of Figures 15 to 17 indicates that the catalysts of Reference Examples 14 to 22 had high conversions both in the initial stage and after the durability test, i.e., exhibited superior durability to the catalysts of Conventional Examples 3 to 11. This is supposed to be an effect of loading Pt and Rh as a composite colloid. Especially the catalysts of Reference Examples 14 to 21 containing 10 to 80 mol% of Rh had higher activity than the catalyst of Reference Example 4 which was a Pt colloid-loaded catalyst. Evidently, this is also an effect of loading Pt and Rh as a composite colloid.

[0099] Especially when the Rh amount was in the range of 30 to 50 mol%, the 50% conversion temperatures were less than 300 °C even after the durability test, which means excellent durability.

## EP 1 043 065 B1

(Reference Example 23)

**[0100]** Figure 18 shows schematic explanatory views showing the change of colloidal particles in the production method of this Reference example.

<Preparation of a Polymer-Protected Noble Metal Composite Colloidal Solution>

**[0101]** 93.9g of polyvinyl pyrrolidone was dissolved into 7700g of water to prepare a uniform solution. 159.40g of a chloroplatinic acid aqueous solution at a Pt concentration of 15.056% by weight, 117.80g of a rhodium chloride aqueous solution at a Rh concentration of 4.606% by weight and 2000g of ethanol were added to this solution and stirred for one hour, thereby preparing a uniform solution.

**[0102]** This solution was heated and after ethanol started reflux, the reflux was continued by heating for eight hours, thereby obtaining a dark brown solution. This solution was concentrated by using a rotary evaporator, thereby obtaining paste. Water was added to this paste to dissolve the paste again, thereby preparing a solution in which a polymer-protected noble metal composite 1 was uniformly dispersed in water. The respective noble metal concentrations of this aqueous solution were measured by ICP (inductively coupled plasma spectrometry). The Pt was 5.12 % by weight and the Rh was 1.16 % by weight (Pt: 70.0 mol%, Rh: 30.0 mol%).

<Ligand Substitution>

**[0103]** To prepare a uniform aqueous solution, 800g of water was added to 6.51g of the obtained polymer-protected noble metal composite colloid aqueous solution which contained 2.44mmol in total of the noble metals. The whole of this aqueous solution, and a solution of 9.61g (36.6mmol, fifteen times of the total amount of noble metals) of triphenyl phosphine ((C<sub>6</sub>H<sub>5</sub>)<sub>3</sub>P) was dissolved in 1000g of toluene were introduced into a separating funnel. The funnel was vigorously shaken for one hour and then left quiet for 24 hours. Thus the content was separated into a transparent water layer (a lower layer) and a black flocculent substance-floating organic layer (an upper layer). So, the water layer was removed.

**[0104]** Then 800g of water was added to the remaining organic layer and the mixture was vigorously shaken for fifteen minutes and then left quiet and the separated water layer was removed. This water cleansing step was carried out five times in order to remove water-soluble impurities. The obtained material was a ligand-protected noble metal composite colloid 2 shown in Figure 18. Then, 200g of acetone was added to this colloid, shaken vigorously and left quiet. Since black powdery substance deposited, the liquid layer was removed quietly. This acetone cleansing step was repeated five times so as to remove acetone-soluble impurities. The black powdery substance thus obtained was transferred into a 100ml reagent bottle. 50g of acetone was added into the bottle and treated by an ultrasonic cleaner for 10 minutes. Then acetone as the supernatant liquid was removed quietly. This ultrasonic cleansing step was repeated two times, thereby obtaining noble metal composite colloidal particles 3.

<Protection by a Surfactant>

**[0105]** While an ultrasonic treatment was applied to the obtained noble metal composite colloidal particles, 1.06g of sodium lauryl sulfate (CH<sub>3</sub>(CH<sub>2</sub>)<sub>11</sub>OSO<sub>3</sub>Na) as an anionic surfactant was added to the colloidal particles and at the same time water was added until it becomes a solution in which noble metal composite colloidal particles were uniformly dispersed in water. Thus, a solution was prepared in which a surfactant-protected noble metal composite colloid 4 was uniformly dispersed. The respective noble metal concentrations of this solution were measured by the ICP. Pt was 0.64% by weight and Rh was 0.15% by weight. This solution was a pure uniform solution which didn't give sediment even after left for one month at room temperature.

(Reference Example 24)

**[0106]** A surfactant-protected noble metal composite colloidal solution was prepared in the same way as that of Reference Example 23 except that 0.97g of lauryl trimethyl ammonium chloride ([CH<sub>3</sub>(CH<sub>2</sub>)<sub>11</sub>N(CH<sub>3</sub>)<sub>3</sub>]Cl) as a cationic surfactant was used instead of sodium lauryl sulfate. The respective noble metal concentrations of this solution were measured by the ICP. Pt was 0.74% by weight and Rh was 0.17% by weight. This solution was a pure uniform solution which didn't give sediment even after left for one month at room temperature.

(Reference Example 25)

**[0107]** A surfactant-protected noble metal composite colloidal solution was prepared in the same way as that of

# EP 1 043 065 B1

Reference Example 23 except that 1.40g of polyethylene glycol lauryl ether ( $\text{CH}_3(\text{CH}_2)_{11}(\text{OCH}_2\text{CH}_2)_n\text{OH}$ ,  $n \approx 9$ ) as a nonionic surfactant was employed instead of sodium lauryl sulfate. The respective noble metal concentrations of this solution were measured by the IPC. Pt was 0.71 % by weight and Rh was 0.16% by weight. This solution was a pure uniform solution which didn't give sediment even after left for one month at room temperature.

(Reference Example 26)

**[0108]** A surfactant-protected noble metal composite colloidal solution was prepared in the same way as that of Reference Example 23, except that 0.63g of  $\beta$ -N-lauryl amino propionic acid ( $\text{CH}_3(\text{CH}_2)_{11}\text{NH}_2\text{CH}_2\text{CH}_2\text{COOH}$ ) as an amphoteric surfactant was employed instead of sodium lauryl sulfate. The respective noble metal concentrations of this solution were measured by the IPC. Pt was 0.68% by weight and Rh was 0.15% by weight. This solution was a pure uniform solution which didn't give sediment even after left for one month at room temperature.

(Reference Example 27)

**[0109]** The Pt-Rh composite colloidal solution (Pt: 90mol%, Rh: 10mol%) synthesized in Reference Example 14 was regarded as Reference Example 27. This colloidal solution was a polymer-protected noble metal composite colloidal solution.

<Experiment 5>

**[0110]** The colloidal solutions of Reference Examples 23 to 27 were diluted with water to contain 0.050g of Pt and 0.011g of Rh. The pH of the solutions were controlled as shown in Table 3 by using nitric acid or aqueous ammonia, if necessary.

**[0111]** On the other hand, test pieces were prepared by coating 0.43g of each porous oxide support powder of  $\gamma\text{-Al}_2\text{O}_3$  powder,  $\text{TiO}_2$  powder and  $\text{ZrO}_2$  powder on a honeycomb-shaped monolith supporting base material formed of cordierite and having a diameter of 30mm, a height of 50mm and a capacity of 35.5ml. The test pieces were respectively immersed in 70ml of the above solutions. Then time to decrease the noble metal concentration of the supernatant to one hundredth of the initial values was respectively measured and the results are shown in Table 3. The measurement was done at one hour intervals from 0 to 12 hours and 12 hours intervals after 12 hours. When the solutions were short, the solutions were synthesized again by the respective methods of Examples and Comparative Examples.

<Evaluation>

**[0112]**

[Table 3]

|           | pH | TIME TO DECREASE CONCENTRATION TO 1/100 OR LESS (hr) |                 |                  |
|-----------|----|--|-----------------|------------------|
|           |    | ALUMINA SUPPORT                                      | TITANIA SUPPORT | ZIRCONIA SUPPORT |
| Ref.Ex.23 | 4  | 3  | 4               | 4                |
| Ref.Ex.24 | 10 | 4  | 5               | 5                |
| Ref.Ex.25 | 4  | 7  | 8               | 8                |
| Ref.Ex.25 | 7  | 7  | 8               | 8                |
| Ref.Ex.25 | 10 | 7  | 8               | 8                |
| Ref.Ex.26 | 4  | 3  | 4               | 4                |
| Ref.Ex.26 | 7  | 6  | 7               | 7                |
| Ref.Ex.26 | 10 | 3  | 4               | 4                |
| Ref.Ex.27 | 4  | 60   | 72              | 72               |
| Ref.Ex.27 | 7  | 60   | 72              | 72               |
| Ref.Ex.27 | 10 | 60   | 72              | 72               |

**[0113]** It is appreciated from Table 3 that the respective colloidal solutions of Reference examples 23 to 26 were

remarkably improved in the adsorption rate of the noble metal composite colloid on the support when compared with the colloidal solution of Reference Example 27. It is evident that the adsorption ability of the noble metal composite colloid on the support was greatly improved by using a surfactant-protected noble metal composite colloidal solution instead of a polymer-protected noble metal composite colloidal solution.

**[0114]** Moreover, it is apparent that in the case of employing such an amphoteric surfactant as that of Reference Example 26, the adsorption rates of the noble metal composite colloid were changed by pH control. It is also apparent that the adsorption rates could be improved by changing the electrostatic characteristics of the colloidal surface.

**[0115]** It is also seen from the different adsorption rates depending on the kind of supports that when the production method of the present invention was carried out by using a support mixture comprising plural kinds of powdery supports, different kinds of noble metals could be loaded easily in accordance with the kind of supports.

(Example 1)

**[0116]** Figure 19 schematically shows an exhaust-gases-purifying catalyst of this example. This catalyst comprises alumina 5 as a porous oxide support, a Pt-Rh composite colloid 6 loaded on the alumina 5, and barium carbonate 7 as an NO<sub>x</sub> storage component loaded on the alumina 5.

**[0117]** Hereinafter, the production method of this catalyst will be explained instead of giving detailed description of the arrangement.

**[0118]** First, 40g of  $\gamma$ -Al<sub>2</sub>O<sub>3</sub> was dispersed in water and 17.03g of barium acetate was added therein. The mixture was concentrated and dried into solids, thereby preparing barium acetate-loaded alumina. 51.33g of this barium acetate-loaded alumina was collected, calcined at 550 °C for two hours and then mixed in a solution of 4.3g ammonium hydrogen carbonate in 300g water and stirred for fifteen minutes. Then the resultant material was filtered under reduced pressure and dried, thereby preparing barium carbonate-loaded alumina.

**[0119]** Next, the barium carbonate-loaded alumina was dispersed in 300g of water. A Pt-Rh composite colloidal solution (Pt: 90mol%, Rh: 10mol%) separately prepared was added to this so that the total mole of Pt and Rh became  $3.42 \times 10^{-3}$  mol. The mixture was stirred for 30 minutes and then filtered to collect powder. This powder was dried at 110 °C for two hours and calcined at 450 °C for two hours, thereby preparing catalyst powder of this example. The total concentration of Pt and Rh loaded was  $9.40 \times 10^{-5}$  mol with respect to 1g of alumina powder, and the concentration of Ba loaded was  $1.67 \times 10^{-3}$  mol with respect to 1g of alumina powder. This catalyst powder was shaped into pellets having particle size of 1 to 3mm and subjected to experiments mentioned later.

(Example 2)

**[0120]** A pellet catalyst of Example 2 was prepared in the same way as that of Example 1, except for the use of a Pt-Rh composite colloidal solution having a different Pt-Rh ratio (Pt: 70mol%, Rh: 30mol%).

(Example 3)

**[0121]** A pellet catalyst of Example 3 was prepared in the same way as that of Example 1, except for the use of a Pt-Rh composite colloidal solution having a different Pt-Rh ratio (Pt: 50mol%, Rh: 50mol%).

(Comparative Example 1)

**[0122]** Figure 20 schematically shows a catalyst of Comparative Example 1. This catalyst comprises alumina 5 as a porous oxide support, Pt 60 and Rh 61 which were loaded on the alumina 5 and highly dispersed on an atomic level, and barium carbonate 7 as an NO<sub>x</sub> storage component loaded on the alumina 5.

**[0123]** This catalyst was produced in the same way as that of Example 1, except that a mixed solution of platinum dinitrodiamine complex and rhodium nitrate was used instead of the Pt-Rh composite colloidal solution (Pt: 90mol%, Rh: 10mol%). The concentrations of Pt and Rh loaded were the same as those of Example 1.

(Comparative Example 2)

**[0124]** A pellet catalyst of Comparative Example 2 was prepared in the same way as that of Example 2, except that a mixed solution of platinum dinitrodiamine complex and rhodium nitrate was used instead of the Pt-Rh composite colloidal solution (Pt: 70mol%, Rh: 30mol%). The concentrations of Pt and Rh loaded were the same as those of Example 2.



# EP 1 043 065 B1

(Comparative Example 3)

**[0125]** A pellet catalyst of Comparative Example 3 was prepared in the same way as that of Example 3, except that a mixed solution of platinum dinitrodiamine complex and rhodium nitrate was used instead of the Pt-Rh composite colloidal solution (Pt: 50mol%, Rh: 50mol%). The concentrations of Pt and Rh loaded were the same as those of Example 17.

<Experiment 6>

**[0126]** The pellet catalysts of Examples 1 to 3 and Comparative Examples 1 to 3 were respectively placed in laboratory reactors and a model exhaust gas with the composition shown in Table 4 was introduced at a space velocity of 100,000h<sup>-1</sup>. Specifically speaking, the constant fuel-lean gas supply was switched to the fuel-rich gas supply for five seconds, and then returned to the fuel-lean gas supply. Three kinds of catalyst bed temperatures, 300 °C, 350 °C and 400°C were selected, and at each temperature the amount of NO<sub>x</sub> adsorbed was measured after a fuel-rich spike (the fuel-rich gas was introduced for five seconds and then the fuel-lean gas was introduced again). The results are shown in Figure 21.

**[0127]** A durability test was carried out by calcining the respective catalysts at 700 °C for ten hours in the air. These catalysts after the durability test were examined about the amount of NO<sub>x</sub> adsorbed in the same way as above. The results are presented in Figure 22.

[Table 4]

|               | H <sub>2</sub> (%) | NO (ppm) | C <sub>3</sub> H <sub>6</sub> (ppm) | CO <sub>2</sub> (%) | CO (ppm) | O <sub>2</sub> (%) | H <sub>2</sub> O (%) | N <sub>2</sub> |
|---------------|--------------------|----------|-------------------------------------|---------------------|----------|--------------------|----------------------|----------------|
| FUEL-LEAN GAS | 0                  | 800      | 1800                                | 11.0                | 0        | 7                  | 3                    | balance        |
| FUEL-RICH GAS | 0.15               | 10       | 1000                                | 11.0                | 6000     | 0                  | 3                    | balance        |

**[0128]** Moreover, regarding the catalysts of Example 1 and Comparative Example 1, the shape of noble metal particles before and after the durability test were observed through an electron microscope. Figure 23 shows a photograph of the catalyst of Example 1 before the durability test. Figure 24 shows a photograph of the catalyst of Example 1 after the durability test. Figure 25 shows a photograph of the catalyst of Comparative Example 1 after the durability test. A photograph of the catalyst of Comparative Example 1 before the durability test is not shown here, because Pt and Rh particles were so small that particle shapes could not be observed.

<Evaluation>

**[0129]** As clear from Figures 21 and 22, in the case of comparing the catalysts of the example and the comparative example which had the same noble metal composition, the catalysts of the examples on which the Pt-Rh composite colloid was loaded had a larger amount of NO<sub>x</sub> adsorbed after a rich spike. This difference was remarkably greater after the durability test and the catalyst of the example was immensely superior in durability. This is supposed to be an effect of loading the noble metals as a noble metal composite colloid.

**[0130]** As evident from Figures 23 to 25, the catalyst of Example 1 had a Pt-Rh particle size as small as about 4nm. As apparent from the fact that the particle size after the durability test was only about 5nm, grain growth during the durability test was very little. In Figures 23 and 24, the projection in the upper right direction is a noble metal composite colloidal particle, and the striped pattern seen in the noble metal composite colloidal particle was the arrangement of the Pt atoms and the Rh atoms, and the blurred portion around the noble metal composite colloidal particle is the distortion of an electronic image. However, in the catalyst of Comparative Example 1, Pt or Rh particles could not be observed before the durability test because of their atomic state, but as Figure 25 shows in its center the rough-triangle material which was a noble metal particle, the particle size grew to about 20 to 25 nm after the durability test.

**[0131]** That is to say, the grain growth of noble metals during the durability test in the catalyst of Example 1 was remarkably suppressed when compared with that of the catalyst of Comparative Example 1, and this fact is supposed to contribute to excellent durability of NO<sub>x</sub> conversion as described above. This is apparently an effect of loading the noble metals as a noble metal composite colloid.

<Experiment 7>

**[0132]** The pellet catalysts of Examples 1 to 3 and Comparative Examples 1 to 3 were placed in laboratory reactors

respectively, and a model exhaust gas with the composition shown in Table 5 was introduced at a space velocity of  $100,000\text{h}^{-1}$ . While the catalyst bed temperature was varied in the range from 25 to 600 °C, 50% conversion temperatures of  $\text{HC}(\text{C}_3\text{H}_6)$ , CO and  $\text{NO}_x$  were measured. The results are shown in Figure 26.

[0133] A durability test was carried out by calcining the respective catalysts at 700 °C for ten hours in the air. The catalysts after the durability test were also examined about 50% conversion temperatures in the same way as above. The results are presented in Figure 27.

[Table 5]

| NO<br>(ppm) | $\text{C}_3\text{H}_6$<br>(ppm) | $\text{CO}_2$<br>(%) | CO<br>(ppm) | $\text{H}_2$<br>(ppm) | $\text{O}_2$<br>(%) | $\text{H}_2\text{O}$<br>(%) | $\text{N}_2$ |
|-------------|---------------------------------|----------------------|-------------|-----------------------|---------------------|-----------------------------|--------------|
| 2400        | 7200                            | 14.4                 | 1200        | 400                   | 0.5                 | 3                           | balance      |

<Evaluation>

[0134] As apparent from Figures 26 and 27, in the case of comparing the catalysts which had the same noble metal composition, the catalysts of the examples had lower 50% conversion temperatures both in the initial stage and after the durability test, that is to say, had a higher catalytic activity. This is supposed to be an effect of loading the noble metals as a noble metal composite colloid.

<Experiment 8>

[0135] The pellet catalysts of Examples 1 to 3 and Comparative Examples 1 to 3 were placed in laboratory reactors respectively, and a gas prepared by adding 100ppm of  $\text{SO}_2$  to each model exhaust gas having the composition shown in Table 4 was introduced at a catalyst bed temperature of 640°C and a gas space velocity of  $100,000\text{h}^{-1}$ . Specifically speaking, a sulfur poisoning durability test was carried out by repeating a cycle comprising 55 seconds of fuel-lean gas supply and 5 seconds of fuel-rich gas supply for four hours. Then elemental analysis was performed on the catalysts after the sulfur poisoning durability test to measure the amount of S in the catalysts. The results are shown in Figure 28.

<Evaluation>

[0136] As seen from Figure 28, in the case of comparing the catalysts which had the same noble metal composition, the catalysts of the examples after the durability test had smaller amounts of S adsorbed, and were greatly suppressed in terms of sulfur poisoning when compared with the catalysts of the comparative examples. This is supposed to be an effect of loading the noble metals as a noble metal composite colloid.

(Example 4)

[0137] Figure 29 shows the micro structure of the exhaust-gases-purifying catalyst of Example 1. Since the Pt-Rh composite colloid 6 of this catalyst had a diameter of about 3nm, when the micro pores of alumina 5 had diameters as small as on the angstrom order, it was difficult to load the Pt-Rh composite colloid 6 in the micro pores 50. Therefore, only barium carbonate 7 was loaded in the micro pores 50.

[0138] However, since there were no noble metals in the vicinity of the barium carbonate loaded in the micro pores 50, HC adsorbed in the micro pores 50 were hardly oxidized. The barium carbonate 7 loaded in the micro pores 50 could not exhibit  $\text{NO}_x$  adsorption and release capability effectively and the barium carbonate 7 could hardly be utilized effectively.

[0139] The exhaust-gases-purifying catalyst of the present example additionally had a noble metal in the atomic state in the micro pores of the alumina. The schematic diagram is shown in Figure 30. This catalyst for purifying exhaust gases comprises alumina 5 as a porous oxide support, a Pt-Rh composite colloid 6 loaded on the surface of the alumina 5, atomic-state Pt 60 and Rh 61 loaded in the micro pores 50 of the alumina 5, and barium carbonate 7 as an  $\text{NO}_x$  storage component loaded on the surface and in the micro pores 50 of the alumina 5. Hereinafter, the method of producing this exhaust-gases-purifying catalyst will be described instead of describing the arrangement in detail.

[0140] 40g of  $\gamma\text{-Al}_2\text{O}_3$  powder was dispersed in 200g of water, and 17.03g of barium acetate was dissolved therein. Then the mixture was concentrated and dried into solids, thereby obtaining barium acetate-loaded alumina powder. Next, this barium acetate-loaded alumina powder was dispersed in a solution of 4.3g ammonium hydrogen carbonate ( $\text{NH}_4\text{HCO}_3$ ) in 300g water. After stirred for fifteen minutes, this mixture was filtered under reduced pressure and dried, thereby preparing barium carbonate-loaded alumina powder.

[0141] This barium carbonate-loaded alumina powder was dispersed in 300g of water. A Pt-Rh composite colloidal

## EP 1 043 065 B1

aqueous solution (Pt: 90mol%, Rh: 10mol%) produced in the same way as that of Example 1 was added to this so that the total mole of Pt and Rh was  $1.54 \times 10^{-3}$  mol and stirred for thirty minutes. 50g of a pyromellitic acid anhydride aqueous solution at a concentration of 0.2 % by weight was added to this dispersed solution and stirred for fifteen minutes. Furthermore, a mixed aqueous solution of platinum dinitrodiamine complex and rhodium nitrate (Pt: 90mol%, Rh: 10mol%) was added so that the total mole of Pt and Rh was  $1.54 \times 10^{-3}$  mol. The mixture was stirred for thirty minutes and filtered under reduced pressure to collect powder.

[0142] This powder was dried at 110 °C for two hours and calcined at 450 °C for two hours, thereby preparing catalyst powder of the present example. The amount of noble metals loaded was  $8.54 \times 10^{-5}$  mol with respect to 1g of  $\gamma\text{-Al}_2\text{O}_3$  powder, and the amount of Ba loaded was  $1.67 \times 10^{-3}$  mol with respect to 1g of  $\gamma\text{-Al}_2\text{O}_3$ .

(Example 5)

[0143] Catalyst powder of Example 5 was prepared in the same way as that of Example 4, except that the Pt-Rh composite colloidal aqueous solution produced in the same way as that of Reference Example 13 and employed here had the composition of 70 mol% Pt and 30 mol% Rh, and that the mixed aqueous solution of platinum dinitrodiamine complex and rhodium nitrate employed here had the composition of 70mol% Pt and 30mol% Rh. The amounts of the respective ingredients loaded were the same as those of Example 4.

(Comparative Example 4)

[0144] The barium carbonate-loaded alumina powder produced in the same way as that of Example 4 was dispersed in 300g of water. A Pt-Rh composite colloidal aqueous solution (Pt: 90mol%, Rh: 10mol%) produced in the same way as that of Example 4 was added to this so that the total mole of Pt and Rh was  $3.08 \times 10^{-3}$  mol. The mixture was stirred for thirty minutes and filtered under reduced pressure to collect powder.

[0145] This powder was dried 110 °C for two hours and then calcined at 450 °C for two hours, thereby preparing catalyst powder of this comparative example. The amount of noble metals loaded was  $8.54 \times 10^{-5}$  mol with respect to 1g of  $\gamma\text{-Al}_2\text{O}_3$  powder.

[0146] This exhaust-gases-purifying catalyst of Comparative Example 4 had the same arrangement as the exhaust-gases-purifying catalyst of Example 15 except that the amounts of noble metals and Ba loaded were different from those of Example 1, and had the structure shown in Figure 29.

(Comparative Example 5)

[0147] Catalyst powder of Comparative Example 5 was prepared in the same way as that of Comparative Example 4, except that a mixed aqueous solution of platinum dinitrodiamine complex and rhodium nitrate (Pt: 90mol%, Rh: 10mol%) was used instead of the Pt-Rh composite colloidal aqueous solution. The amounts of the respective ingredients loaded were the same as those of Comparative Example 4.

[0148] This exhaust-gases-purifying catalyst of Comparative Example 5 had the same arrangement as the exhaust-gases-purifying catalyst of Comparative Example 12, except that the amounts of noble metals and Ba loaded were different from those of Comparative Example 1. The catalyst of Comparative Example 5 had the structure shown in Figure 20.

(Comparative Example 6)

[0149] Catalyst powder of Comparative Example 6 was prepared in the same way as that of Comparative Example 4, except that the Pt-Rh composite colloidal aqueous solution employed had the composition of 70mol% Pt and 30 mol% Rh. The amounts of the respective ingredients loaded were the same as those of Comparative Example 4.

[0150] The exhaust-gases-purifying catalyst of Comparative Example 6 had the same arrangement as the exhaust-gases-purifying catalyst of Example 1, except that the amounts of noble metals and Ba loaded were different from those of Example 1. The catalyst of Comparative Example 17 had the structure shown in Figure 29.

(Comparative Example 7)

[0151] Catalyst powder of Comparative Example 7 was prepared in the same way as that of Comparative Example 4, except that a mixed aqueous solution of platinum dinitrodiamine complex and rhodium nitrate (Pt: 70mol%, Rh: 30mol%) was employed instead of the Pt-Rh composite colloidal aqueous solution. The amounts of the respective ingredients loaded were the same as those of Comparative Example 4.

[0152] This exhaust-gases-purifying catalyst of Comparative Example 7 had the same arrangement as the exhaust-

gases-purifying catalyst of Comparative Example 1, except that the amounts of noble metals and Ba loaded were different from those of Comparative Example 1. The catalyst of Comparative Example 7 had the structure shown in Figure 20.

#### <Experiment 9>

[0153] The catalyst powder of Examples 4 to 5 and Comparative Examples 4 to 7 were shaped into pellets of 1 to 3mm in particle size, and placed respectively in laboratory reactors and a model gas shown in the aforementioned Table 4 was introduced at a gas space velocity of  $100,000\text{h}^{-1}$ . While the catalyst bed temperature was controlled at three levels,  $300^{\circ}\text{C}$ ,  $350^{\circ}\text{C}$  and  $400^{\circ}\text{C}$ , measurement was conducted on the saturated amount of  $\text{NO}_x$  adsorbed after switched from the fuel-rich gas supply to the constant fuel-lean gas supply (the saturated amount of  $\text{NO}_x$  adsorbed). Then measurement was conducted on the amount of  $\text{NO}_x$  adsorbed just after switched from the constant fuel-lean gas supply to the fuel-rich gas supply for five seconds and again to the fuel-lean gas supply (the amount of  $\text{NO}_x$  adsorbed after a fuel-rich spike). Besides, a durability test was conducted by calcining the respective catalysts at  $700^{\circ}\text{C}$  for ten hours in the air, and then the same measurement was also carried out on the catalysts after the durability test.

[0154] Figure 31 shows the saturated amounts of  $\text{NO}_x$  adsorbed of the brandnew catalysts. Figure 32 shows the amounts of  $\text{NO}_x$  adsorbed of the brandnew catalyst after a rich spike. Figure 33 shows the saturated amounts of  $\text{NO}_x$  adsorbed of the catalysts after the durability test. Figure 34 shows the amounts of  $\text{NO}_x$  adsorbed after the rich spike, which the catalysts after the durability test exhibited.

#### <Evaluation>

[0155] As evident from Figure 31, in the case of comparing the catalysts which had the same noble metal composition, the catalysts of the examples on which the Pt-Rh composite colloid, platinum dinitrodiamine complex and rhodium nitrate were loaded simultaneously had larger saturated amounts of  $\text{NO}_x$  adsorbed in the initial stage than the catalysts of the comparative examples. As clear from Figure 32, the catalysts of the examples had larger amounts of  $\text{NO}_x$  adsorbed after the rich spike than the catalysts of the comparative examples. Similar evaluation to these was obtained from Figures 33 and 34, and it is clear that the catalysts of Examples 4 and 5 were excellent also in durability. It is apparent that these effects were caused by loading the Pt-Rh composite colloid and platinum dinitrodiamine complex and rhodium nitrate simultaneously by using pyromellitic acid.

[0156] It is also apparent from the comparison of the comparative examples that the catalysts of Comparative Examples 4, 6 on which the noble metals were loaded as a Pt-Rh composite colloid were remarkably improved in durability than the catalysts of Comparative Examples 5, 7 on which the noble metals were loaded as platinum dinitrodiamine complex and rhodium nitrate.

#### <Experiment 10>

[0157] The pellet catalysts of Examples 4, 5 and Comparative Examples 4 to 7 were respectively placed in laboratory reactors and a model exhaust gas having the composition shown in Table 5 above was introduced at a space velocity of  $100,000\text{h}^{-1}$ . While the catalyst bed temperature was varied in the range from  $25$  to  $600^{\circ}\text{C}$ , the 50% conversion temperatures of  $\text{HC}(\text{C}_3\text{H}_6)$ ,  $\text{CO}$  and  $\text{NO}_x$  were measured. The results are shown in Figure 35.

[0158] Besides, a durability test was carried out by calcining the respective catalysts at  $700^{\circ}\text{C}$  for ten hours in the air, and the catalysts after the durability test were examined about the 50% conversion temperatures in the same way as above. The results are presented in Figure 36.

#### <Evaluation>

[0159] As apparent from Figures 35 and 36, in the case of comparing the catalysts which had the same noble metal composition, the catalysts of Examples 18, 19 and Comparative Examples 4, 6 on which the Pt-Rh composite colloid was loaded had lower 50% conversion temperatures, that is to say, had higher catalytic activity than the catalysts of Comparative Examples 5, 7 on which the noble metals in the atomic state were loaded. It is also clear that the former catalysts had smaller decrease in catalytic activity after the durability test.

[0160] The catalysts of Examples 4, 5 on which the Pt-Rh composite colloid and platinum dinitrodiamine complex and rhodium nitrate were simultaneously loaded by using pyromellitic acid, and the catalysts of Comparative Examples 4, 6 on which only the Pt-Rh composite colloid was loaded exhibited almost the same level results, which were far better than the catalysts of Comparative Examples 5, 7 on which the noble metals were loaded as platinum dinitrodiamine complex and rhodium nitrate. This indicates that the effect of loading noble metals as a noble metal colloid was obtained even when the Pt-Rh composite colloid was loaded simultaneously with platinum dinitrodiamine complex and

rhodium nitrate. This effect is supposed to be caused by loading the Pt-Rh composite colloid on the surface of the support and loading atomic-state Pt and Rh in the micro pores of the support.

# POSSIBLE INDUSTRIAL UTILITY

5

[0161] According to the exhaust-gases-purifying catalysts recited in claim 2, noble metal grain growth during the durability test is suppressed, so the catalytic activity is suppressed from decreasing due to the collapse of time and these catalysts are extremely superior in durability. Sulfur poisoning of the NO<sub>x</sub> storage component is also suppressed.

10

[0162] Moreover, according to the exhaust-gases-purifying catalyst recited in claim 3, HC adsorbed in the micro pores of the support can be oxidized efficiently. According to the exhaust-gases-purifying catalyst recited in claim 4, the NO<sub>x</sub> storage component loaded in the micro pores of the support is utilized effectively, so the NO<sub>x</sub> conversion ability is improved further.

15

[0163] According to the production method recited in claim 6, the exhaust-gases-purifying catalysts recited in claim 3 and claim 4 can be produced with ease. According to the exhaust-gases-purifying method recited in claim 7, catalytic activity is suppressed from decreasing due to the collapse of time and the NO<sub>x</sub> storage ability can be maintained high, so NO<sub>x</sub> conversion ability can be stably maintained high for a long time.

## Claims

20

1. A catalyst for purifying exhaust gases obtainable by loading on a porous oxide support a noble metal composite colloid composed of a plurality of noble metals and having a particle size of from 1 to 5 nm.

25

2. Catalyst according to claim 1, obtainable by loading the noble metal composite colloid on the surface of said porous oxide support and further loading an atomic-state noble metal in micro pores of said porous oxide support.

30

3. Catalyst according to claim 1 or claim 2, obtainable by further loading on said porous oxide support an NO<sub>x</sub> storage component selected from the group consisting of alkali metals, alkaline-earth metals and rare-earth elements.

35

4. Catalyst according to claim 3, wherein the NO<sub>x</sub> storage component is loaded in micro pores of said porous oxide support.

40

5. A method of producing an exhaust-gases-purifying catalyst, characterized in comprising:

45

a separation step of taking a noble metal composite colloid composed of a plurality of noble metals and having a particle size of from 1 to 5 nm out of a polymer-protected noble metal composite colloid which is composed of a plurality of noble metals and protected by a polymeric material;

50

a solution preparation step of dispersing said noble metal composite colloid in water by using a surfactant so as to prepare a surfactant-protected noble metal composite colloidal solution; and

55

a noble-metal-colloid-loading step of bringing a porous oxide support in contact with said surfactant-protected noble metal composite colloidal solution so as to load a surfactant-protected noble metal composite colloid on said porous oxide support.

60

6. A method of producing an exhaust-gases-purifying catalyst, according to claim 5, further comprising:

65

an atomic-state-noble-metal-loading step of bringing said porous oxide support in contact with an aqueous solution of pyromellitic acid and a noble metal compound so as to load an atomic-state noble metal on said porous oxide support.

70

7. A method of purifying exhaust gases characterized in placing, in exhaust gases in oxygen-excessive atmospheres, a catalyst obtainable by loading on a porous oxide support a noble metal composite colloid composed of a plurality of noble metals and having a particle size of from 1 to 5 nm and an NO<sub>x</sub> storage component selected from the group consisting of alkali metals, alkaline-earth metals and rare-earth elements so as to adsorb NO<sub>x</sub> in said exhaust gases on said NO<sub>x</sub> storage component, and changing the exhaust gas atmospheres to the stoichiometric point or on the fuel-rich side so as to release said NO<sub>x</sub> from said NO<sub>x</sub> storage component and reduce said NO<sub>x</sub>.

Patentansprüche

1. Katalysator zur Reinigung von Abgasen, der erhältlich ist indem ein Edelmetallmischkolloid, das aus einer Vielzahl an Edelmetallen besteht und eine Teilchengröße von 1 bis 5 nm aufweist, auf einen porösen Oxidträger geladen wird.
2. Katalysator nach Anspruch 1, der erhältlich ist, indem das Edelmetallmischkolloid auf die Oberfläche des porösen Oxidträgers geladen wird und ferner ein Edelmetall in atomarem Zustand in Mikroporen des porösen Oxidträgers geladen wird.
3. Katalysator nach Anspruch 1 oder Anspruch 2, der erhältlich, indem ferner eine NO<sub>x</sub>-Speicherkomponente, die aus der aus Alkalimetallen, Erdalkalimetallen und Seltenerdelementen bestehenden Gruppe ausgewählt ist, auf den porösen Oxidträger geladen wird.
4. Katalysator nach Anspruch 3, wobei die NO<sub>x</sub>-Speicherkomponente in Mikroporen des porösen Oxidträgers geladen wird.
5. Verfahren zur Herstellung eines Abgasreinigungskatalysators, **dadurch gekennzeichnet, daß** es folgendes umfaßt:
  - einen Trennungsschritt des Entnehmens eines Edelmetallmischkolloids, das aus einer Vielzahl an Edelmetallen besteht und eine Teilchengröße von 1 bis 5 nm aufweist, aus einem Polymer-geschützten Edelmetallmischkolloid, das aus einer Vielzahl an Edelmetallen besteht und durch ein Polymermaterial geschützt ist;
  - einen Lösungsherstellungsschritt des Dispergierens des Edelmetallmischkolloids in Wasser unter Verwendung eines Tensids, um so eine kolloidale Lösung einer Tensid-geschützten Edelmetallmischung herzustellen; und
  - einen Edelmetallkolloidbeladungsschritt des In-Kontakt-Bringens eines porösen Oxidträgers mit der kolloidalen Lösung einer Tensid-geschützten Edelmetallmischung, um so ein Tensid-geschütztes Edelmetallmischkolloid auf den porösen Oxidträger zu laden.
6. Verfahren zur Herstellung eines Abgasreinigungskatalysators nach Anspruch 5, das ferner folgendes umfaßt:
  - einen Beladungsschritt mit Edelmetall in atomarem Zustand des In-Kontakt-Bringens des porösen Oxidträgers mit einer wäßrigen Lösung von Pyromellithsäure und einer Edelmetallverbindung, um so ein Edelmetall in atomarem Zustand auf den porösen Oxidträger zu laden.
7. Verfahren zur Reinigung von Abgasen, **dadurch gekennzeichnet, daß** ein Katalysator, der erhältlich ist, indem ein Edelmetallmischkolloid, das aus einer Vielzahl an Edelmetallen besteht und eine Teilchengröße von 1 bis 5 nm und eine NO<sub>x</sub>-Speicherkomponente, die aus der aus Alkalimetallen, Erdalkalimetallen und Seltenerdelementen bestehenden Gruppe ausgewählt ist, aufweist, auf einen porösen Oxidträger geladen wird, in einer sauerstoffreichen Atmosphäre in Abgase gegeben wird, um so NO<sub>x</sub> in den Abgasen auf der NO<sub>x</sub>-Speicherkomponente zu adsorbieren, und die Abgasatmosphäre zum stöchiometrischen Punkt oder auf die kraftstoffreiche Seite zu ändern, um so das NO<sub>x</sub> von der NO<sub>x</sub>-Speicherkomponente freizusetzen und das NO<sub>x</sub> zu reduzieren.

Revendications

1. Catalyseur pour purifier les gaz d'échappement disponible en chargeant sur un support oxyde poreux un colloïde composite de métal noble composé d'une pluralité de métaux nobles et ayant une taille de particule allant de 1 à 5 nm.
2. Catalyseur selon la revendication 1, disponible en chargeant le colloïde composite de métal noble sur la surface dudit support oxyde poreux et en chargeant, en outre, un métal noble à l'état atomique dans les micro-pores dudit support oxyde poreux.
3. Catalyseur selon la revendication 1 ou la revendication 2, disponible en chargeant, en outre, sur ledit support

## EP 1 043 065 B1

oxyde poreux un composant de stockage de  $\text{No}_x$  choisi parmi le groupe se composant des métaux alcalins, des métaux alcalino-terreux et des éléments de terre rare.

- 5 4. Catalyseur selon la revendication 3, dans lequel le composant de stockage de  $\text{No}_x$  est chargé dans les micropores dudit support oxyde poreux.
5. Procédé de production d'un catalyseur de purification des gaz d'échappement, caractérisé dans le fait de comprendre :
- 10 une étape de séparation consistant à prendre un colloïde composite de métal noble composé d'une pluralité de métaux nobles et ayant une taille de particule de 1 à 5 nm hors d'un colloïde composite de métal noble protégé par un polymère qui est composé d'une pluralité de métaux nobles et qui est protégé par un matériau polymère ;
- 15 une étape de préparation de solution consistant à disperser ledit colloïde composite de métal noble dans l'eau en utilisant un tensioactif de sorte à préparer une solution colloïdale composite de métal noble protégée par un polymère ; et
- 20 une étape de chargement du colloïde de métal noble consistant à mettre un support oxyde poreux en contact avec ladite solution colloïdale composite de métal noble protégée par un tensioactif de sorte à charger un colloïde composite de métal noble protégé par un tensioactif sur ledit support oxyde poreux.
6. Procédé de production d'un catalyseur de purification des gaz d'échappement, selon la revendication 5, comprenant en outre :
- 25 une étape de chargement du métal noble à l'état atomique consistant à mettre ledit support oxyde poreux en contact avec une solution aqueuse d'acide pyromellique et avec un composé de métal noble protégée de sorte à charger un métal noble à l'état atomique sur ledit support oxyde poreux.
- 30 7. Procédé de purification des gaz d'échappement caractérisé dans le fait de placer, dans les gaz d'échappement dans les atmosphères avec trop d'oxygène, un catalyseur disponible en chargeant sur un support oxyde poreux un colloïde composite de métal noble composé d'une pluralité de métaux nobles et ayant une taille de particule allant de 1 à 5 nm et un composant de stockage de  $\text{No}_x$  choisi parmi le groupe se composant des métaux alcalins, des métaux alcalino-terreux et des métaux de terre rare de sorte à adsorber le  $\text{NO}_x$  dans lesdits gaz d'échappement
- 35 sur ledit composant de stockage de  $\text{No}_x$  et en changeant les atmosphères de gaz d'échappement au point stoechiométrique ou sur le côté riche en carburant de sorte à libérer ledit  $\text{No}_x$  dudit composant de stockage de  $\text{No}_x$  et à réduire ledit  $\text{No}_x$ .
- 40
- 45
- 50
- 55

FIG. 1

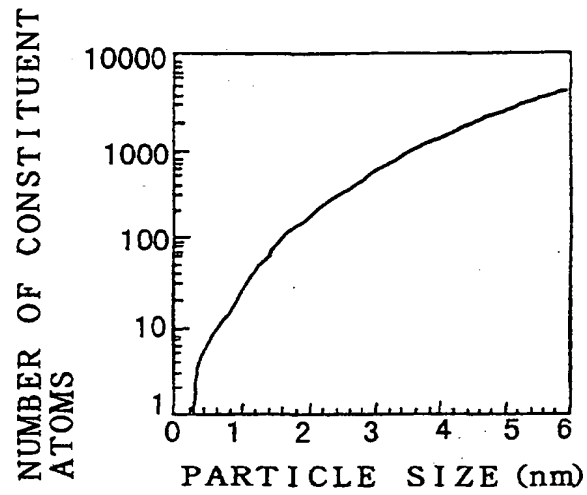


FIG. 2

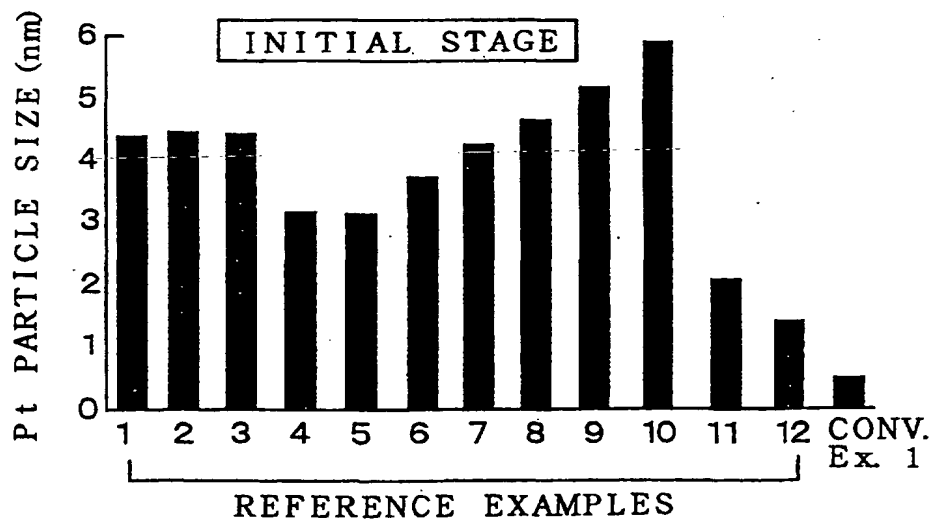




FIG. 3

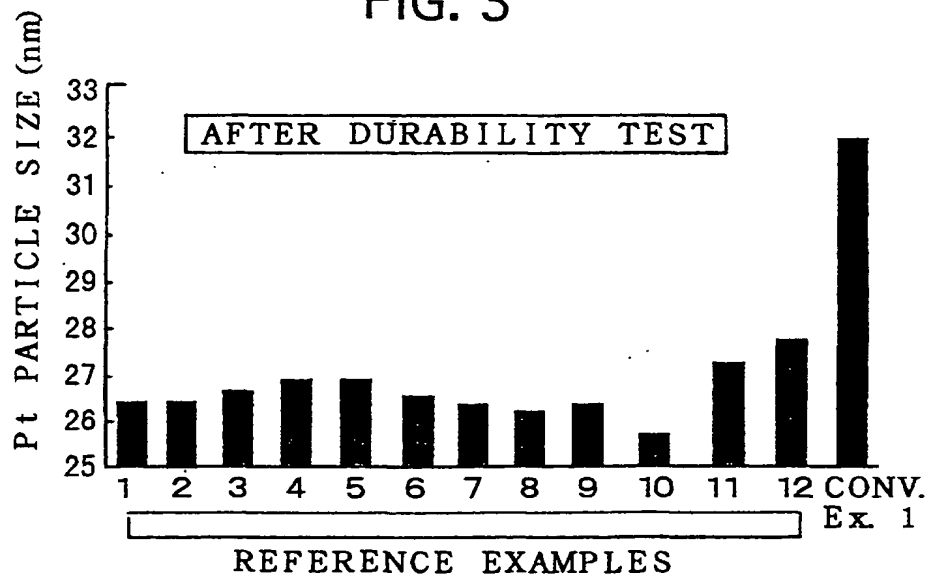


FIG. 4

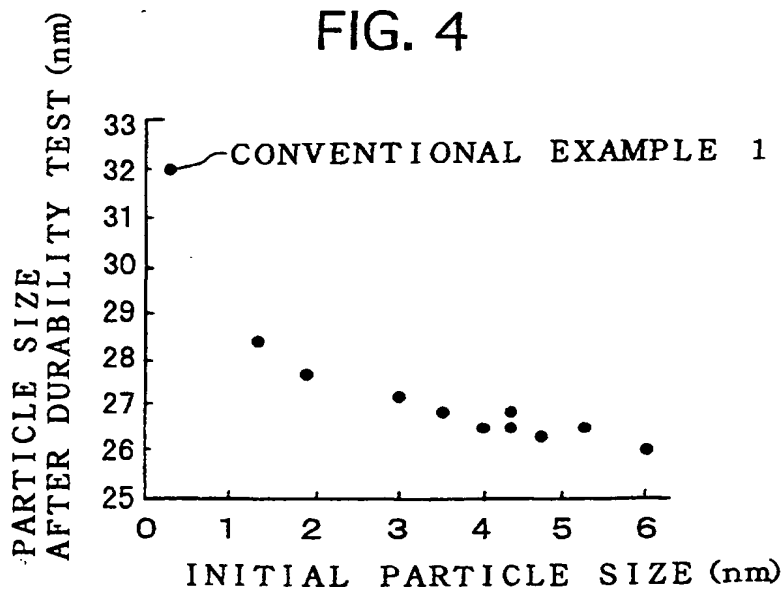


FIG. 5

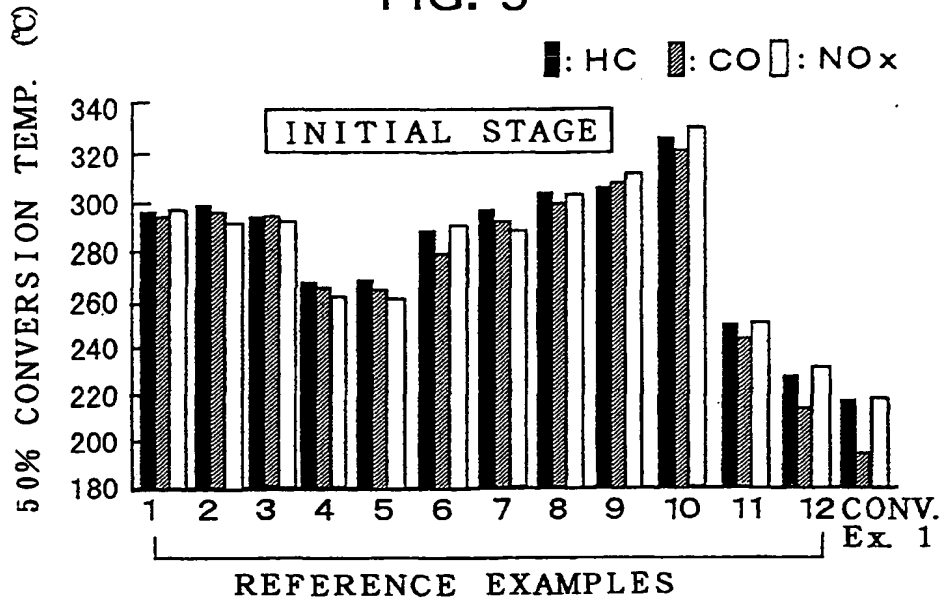


FIG. 6

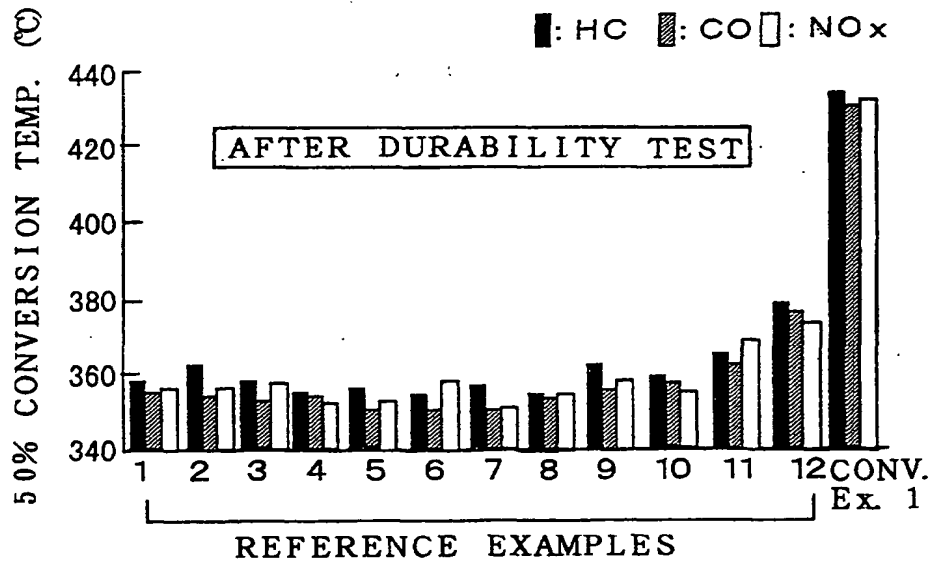


FIG. 7

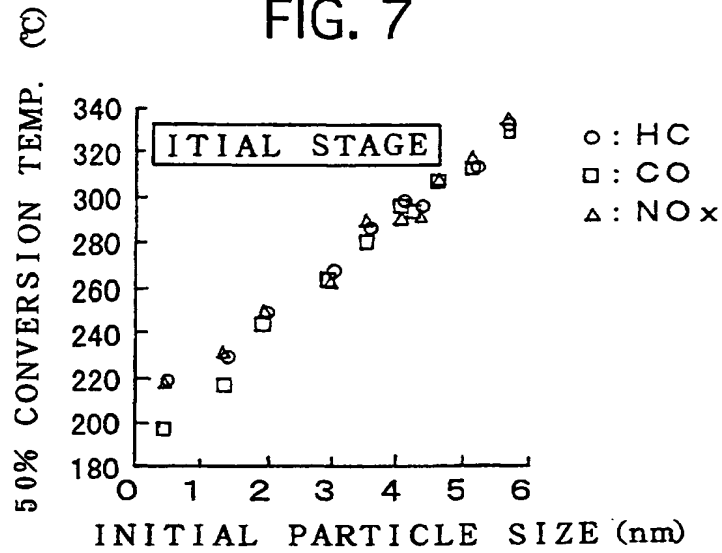
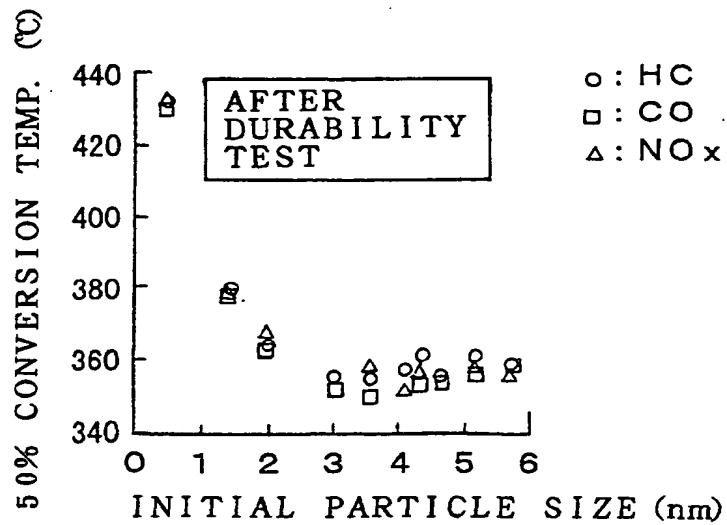


FIG. 8



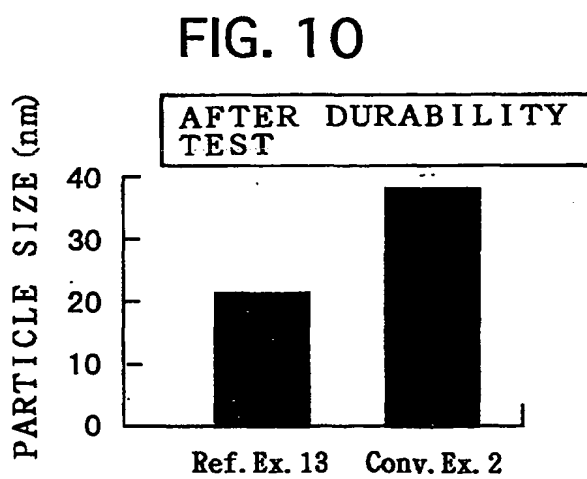
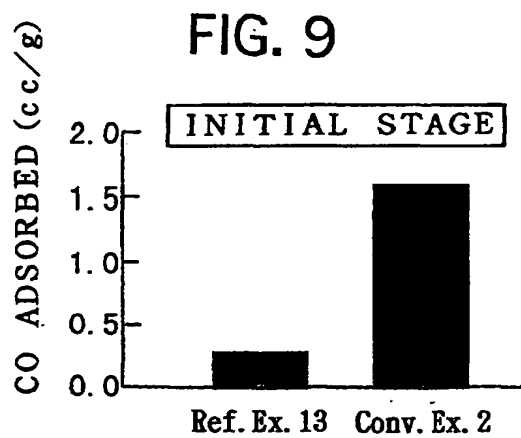


FIG. 11

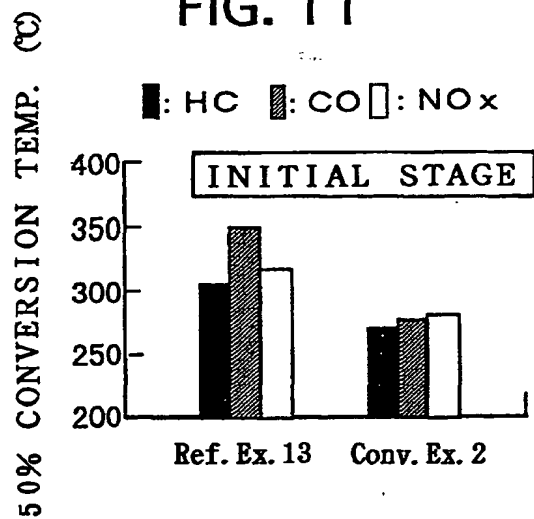


FIG. 12

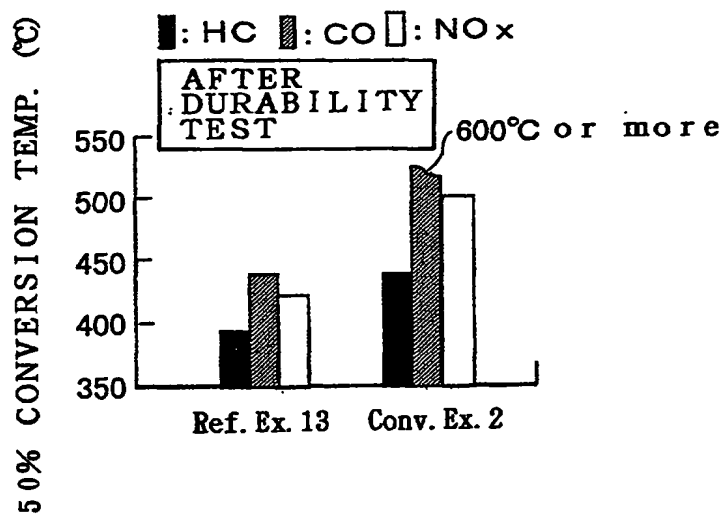


FIG. 13

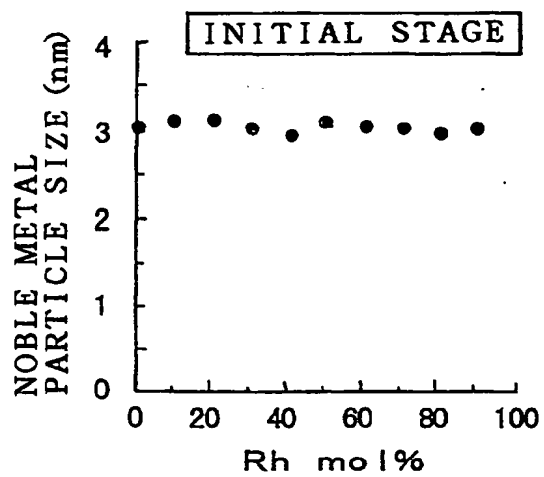


FIG. 14

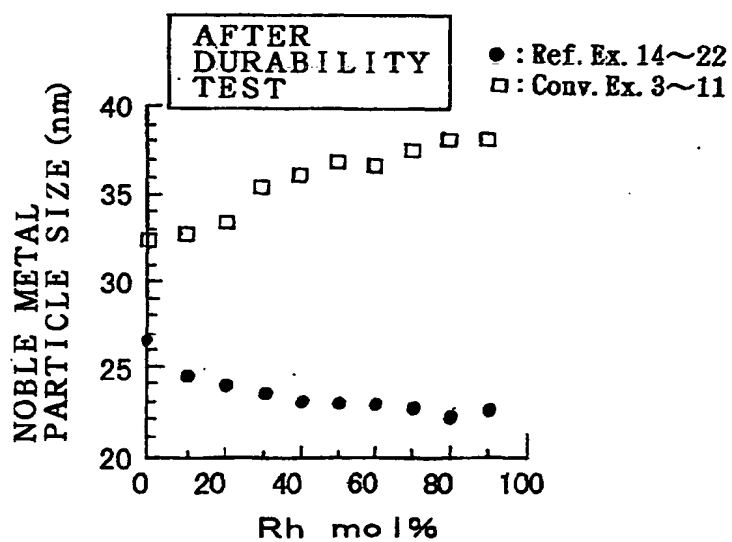


FIG. 15

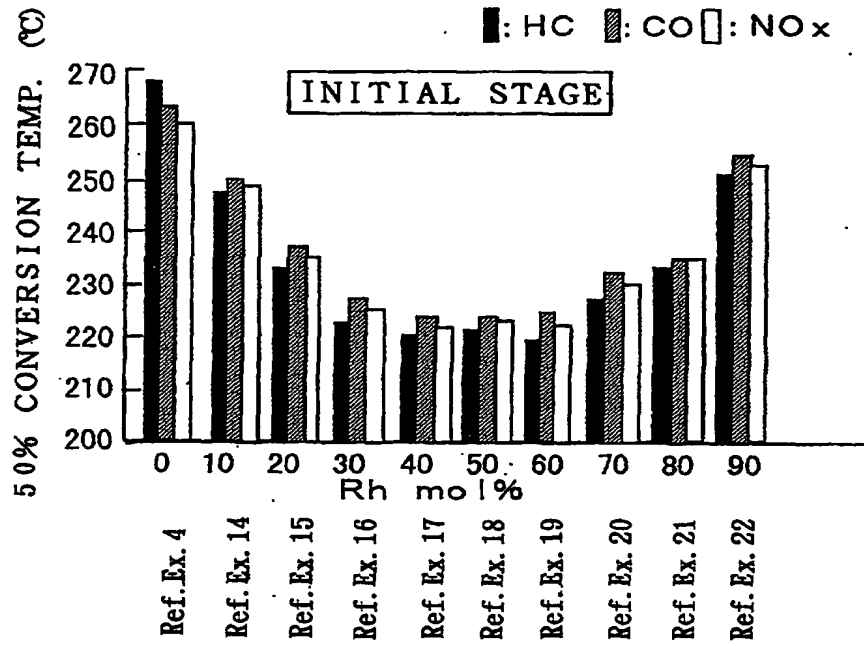


FIG. 16

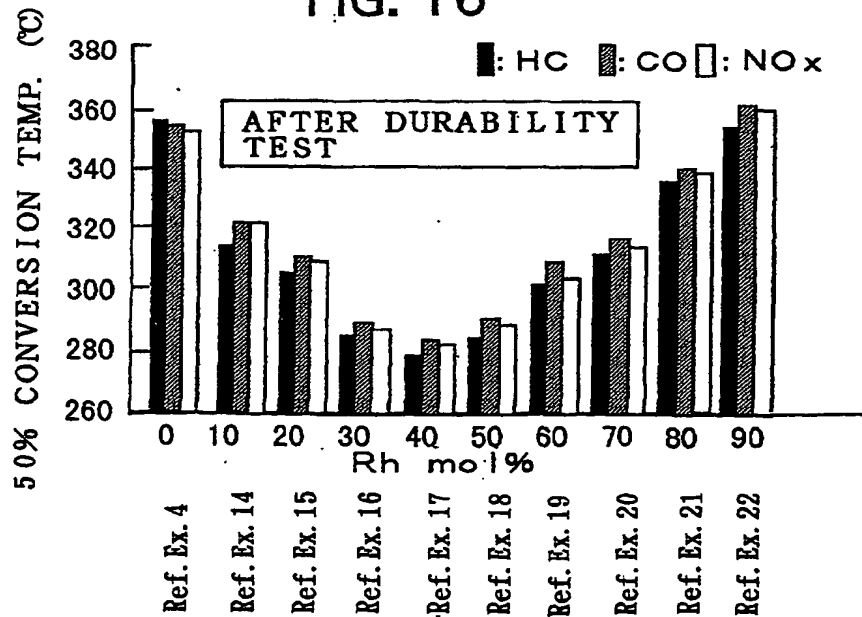


FIG. 17

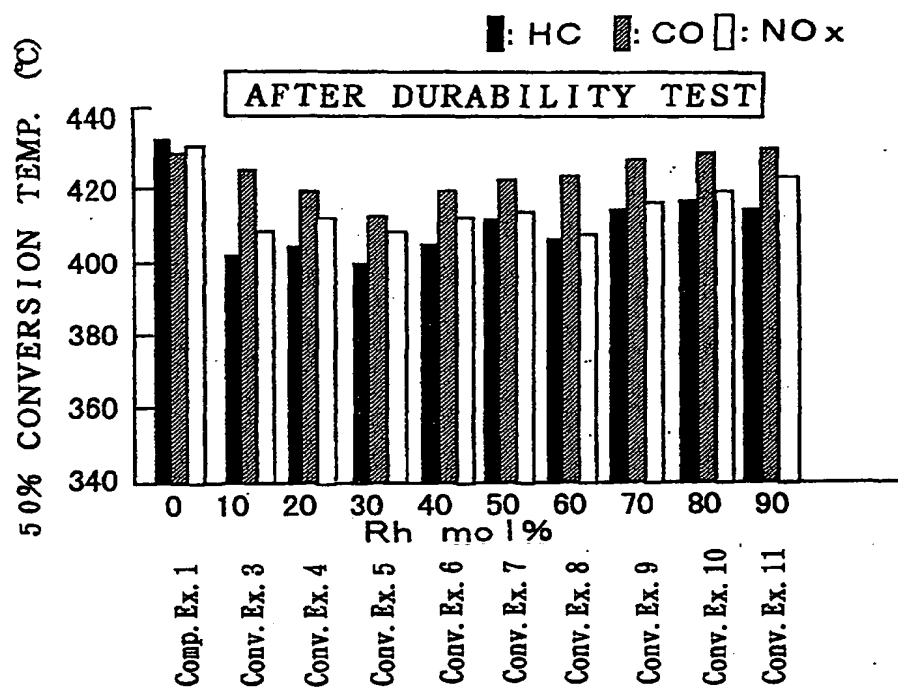




FIG. 18

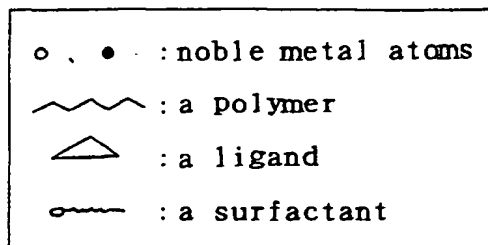
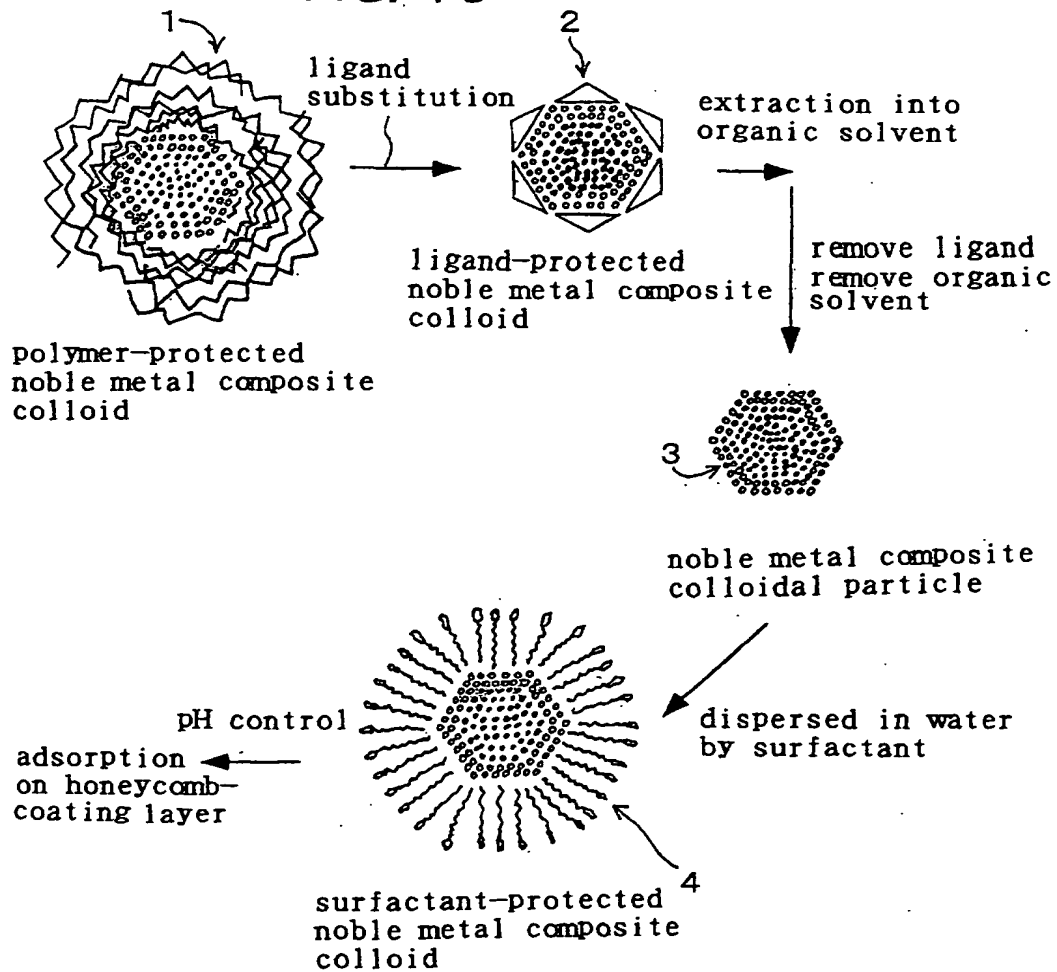


FIG. 19

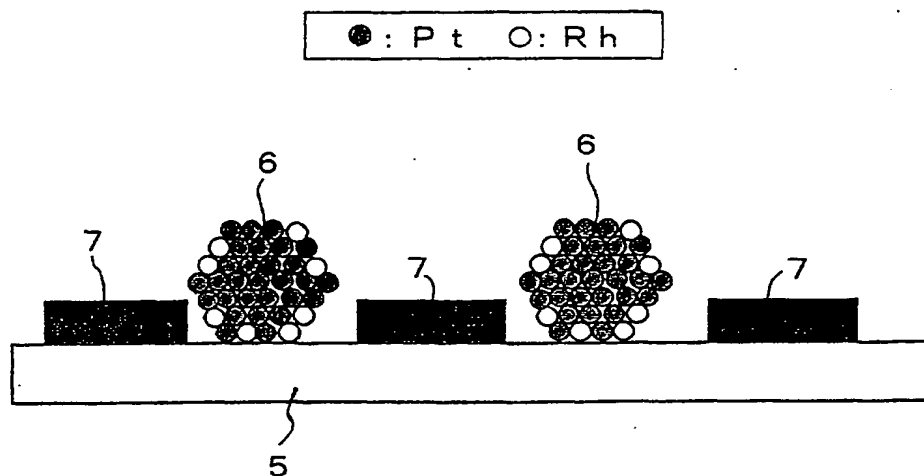


FIG. 20

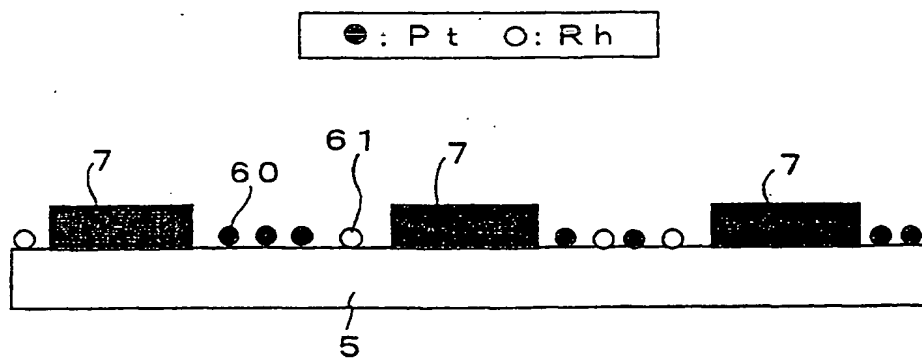


FIG. 21

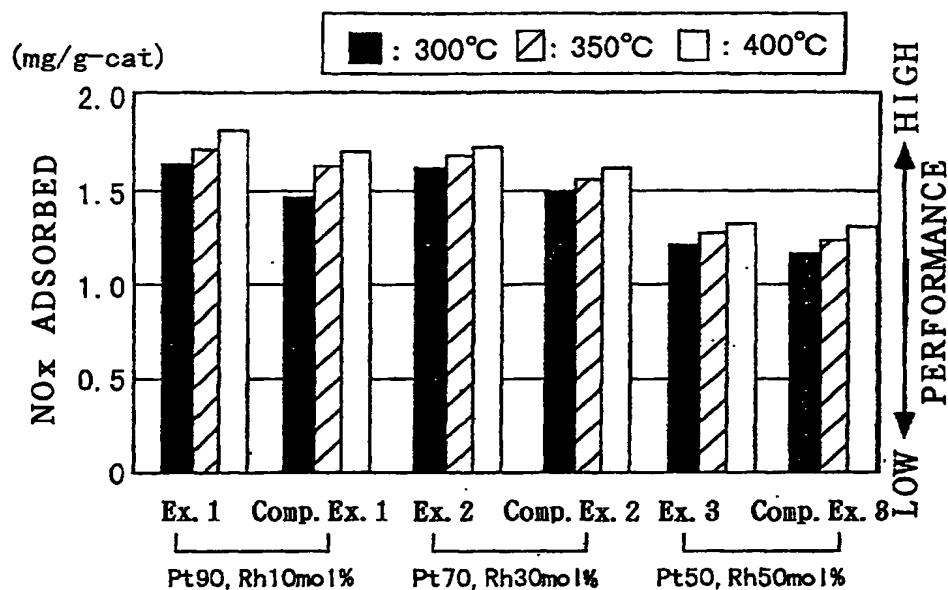


FIG. 22

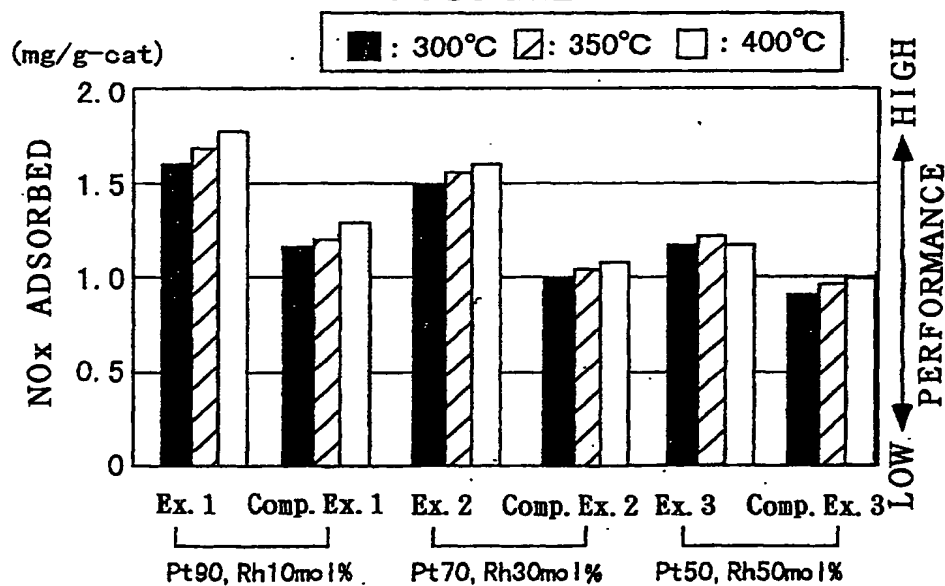
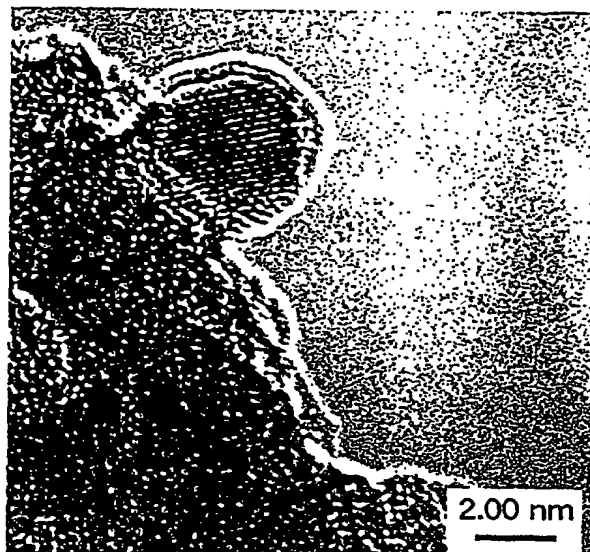
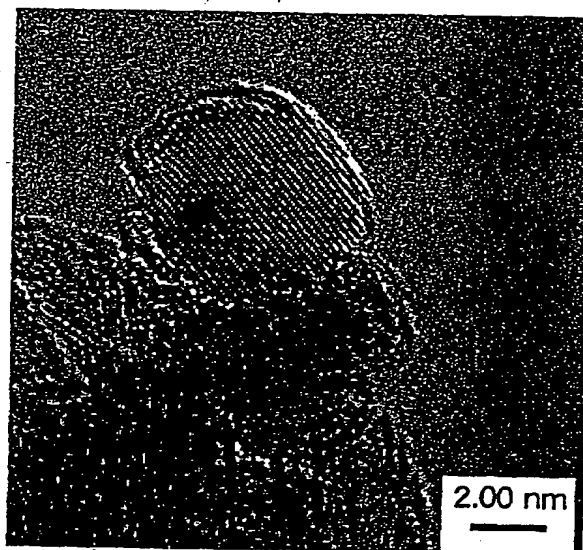


FIG. 23



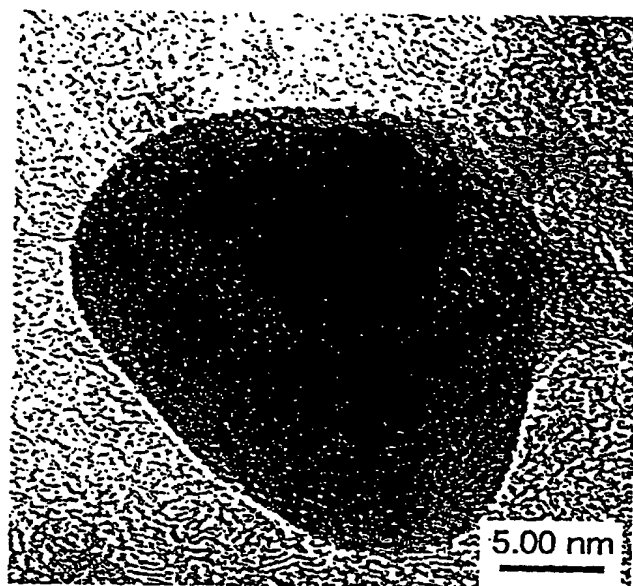
EX. 1 BEFORE  
DURABILITY TEST

FIG. 24



EX. 1 AFTER  
DURABILITY TEST

FIG. 25



Comp. Ex. 1 AFTER  
DURABILITY TEST

FIG. 26

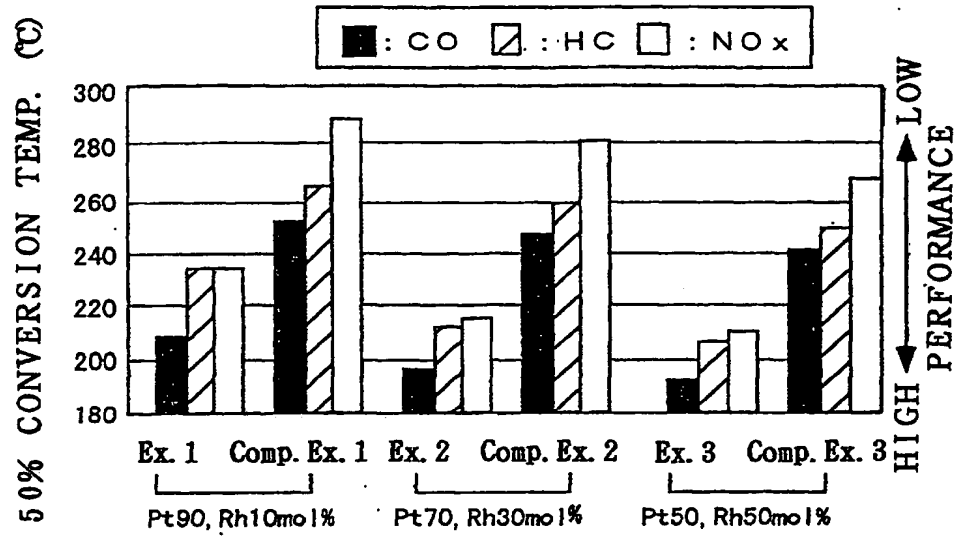


FIG. 27

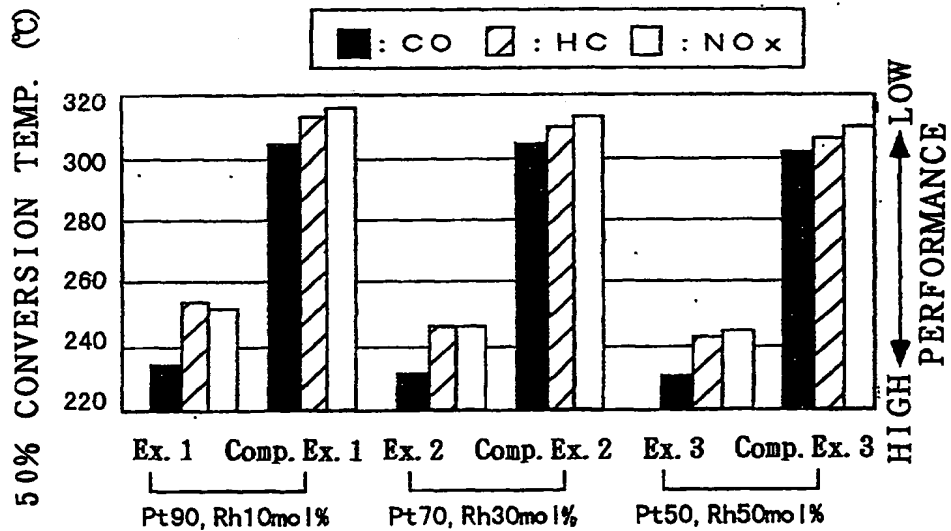


FIG. 28

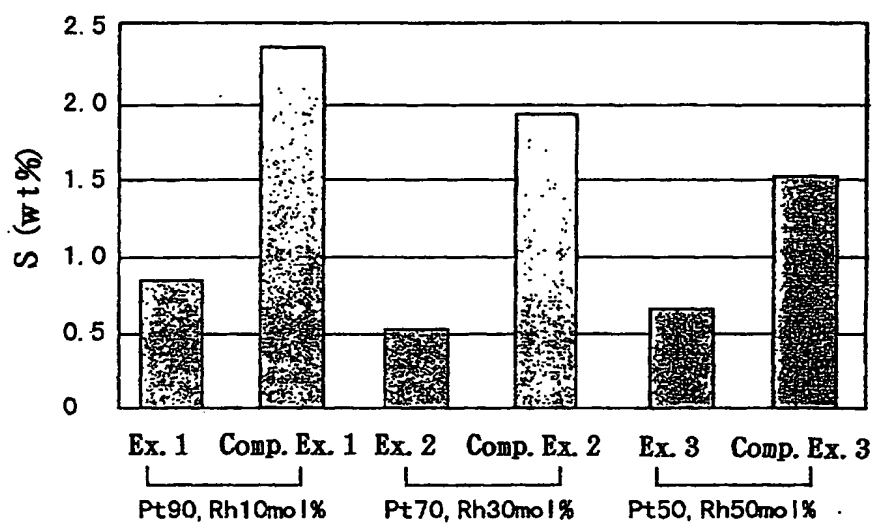


FIG. 29

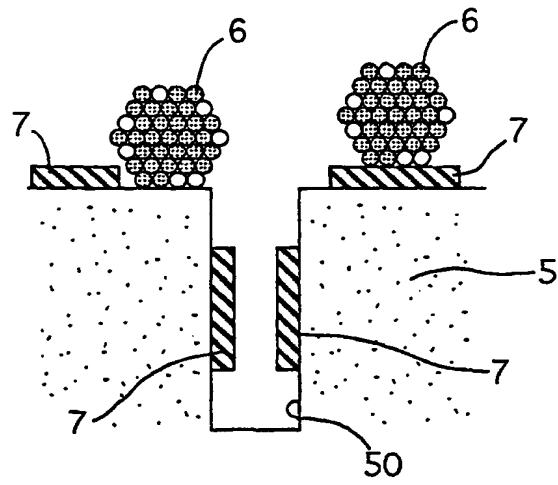


FIG. 30

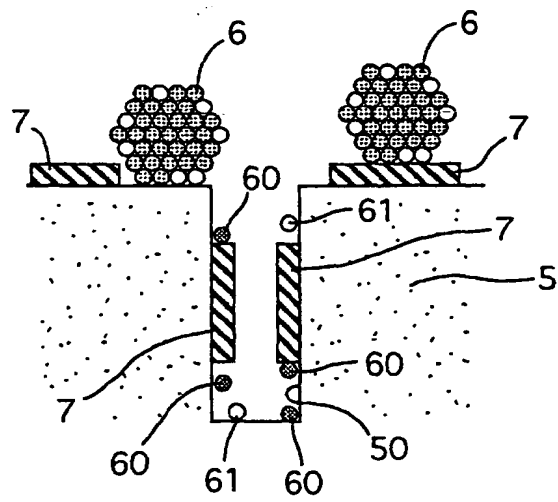




FIG. 31

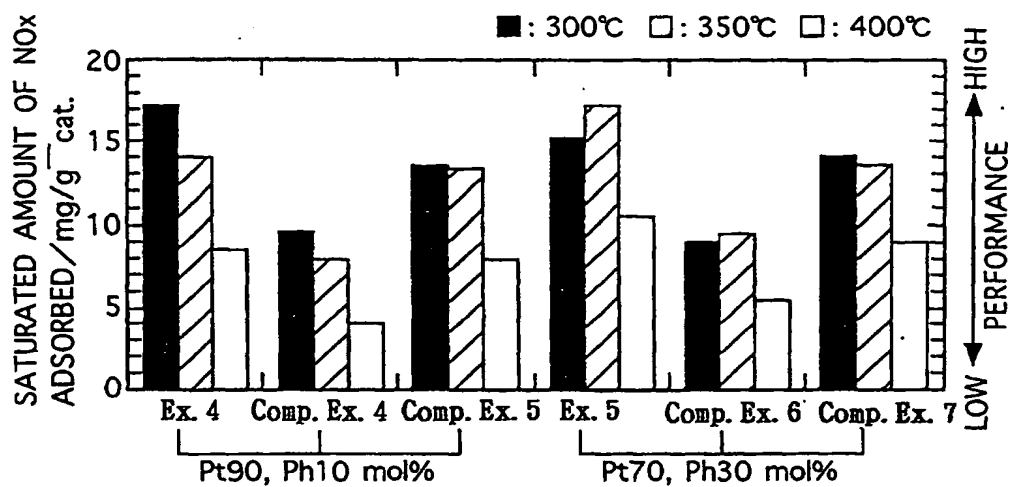


FIG. 32

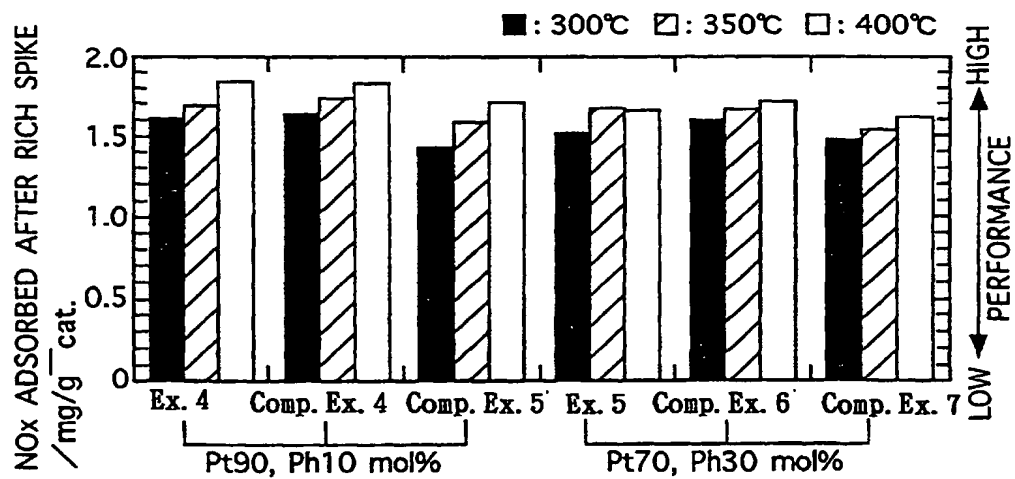


FIG. 33

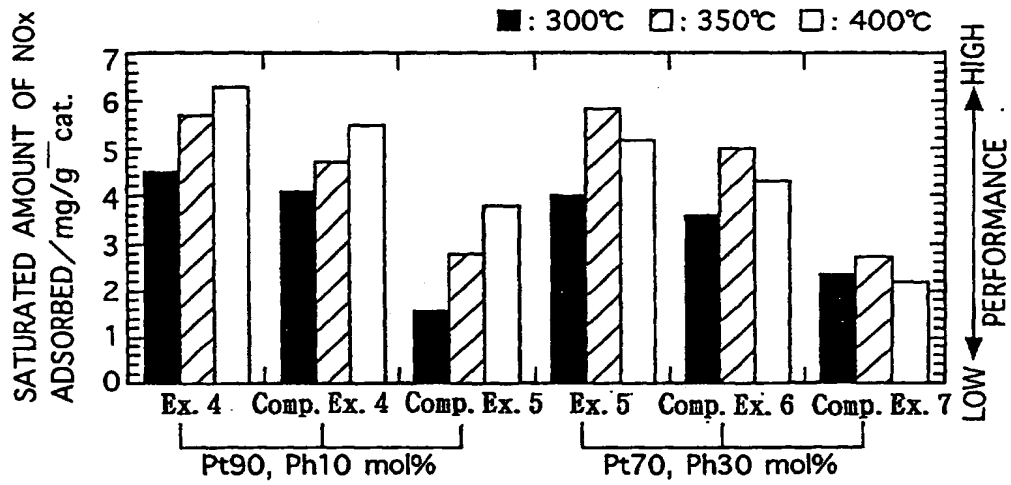


FIG. 34

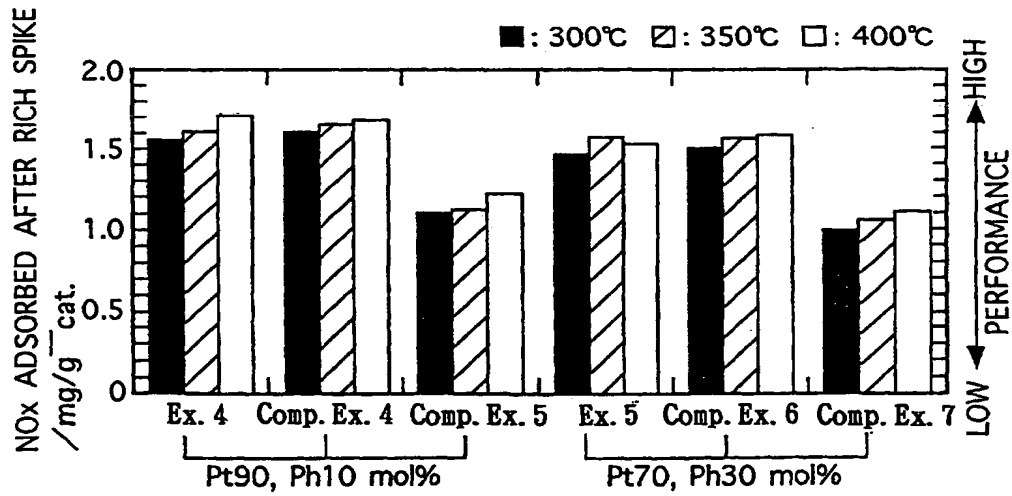


FIG. 35

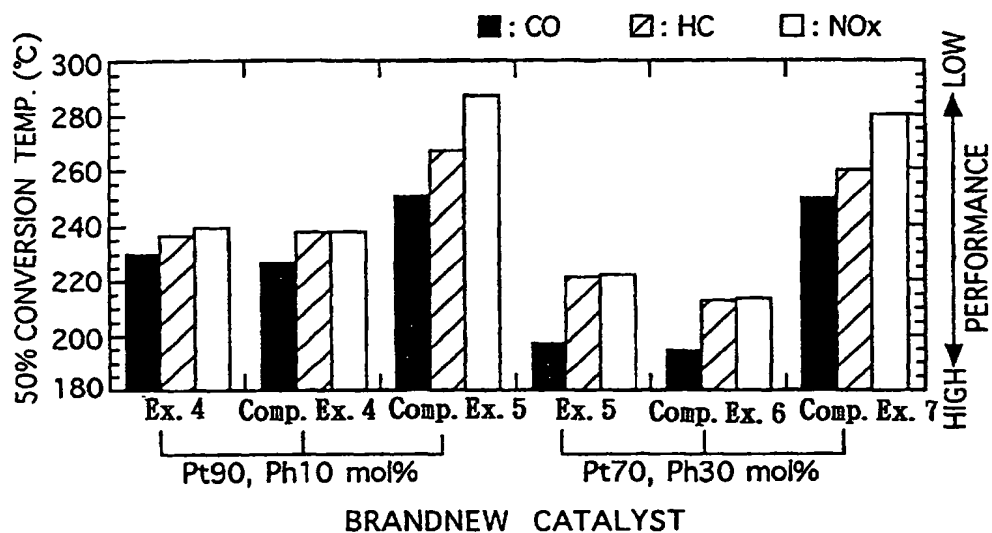


FIG. 36

